Available online at www.sciencedirect.com
SCIENCE DIRECT®
Sedimentary Geology 166 (2004) 157–183
Sedimentary Geology
www.elsevier.com/locate/sedgeo

Using geochemistry to establish the igneous provenances of the Neogene continental sedimentary rocks in the Central Depression and Altiplano, Central Andes

Luisa Pinto[a,*], Gérard Hérail[b], Bernard Moine[c], François Fontan[c], Reynaldo Charrier[a], Bernard Dupré[c]

[a] *Departamento de Geología, Universidad de Chile, Casilla 13518, Correo 21, Santiago, Chile*
[b] *IRD-LMTG, 38 rue des 36 Ponts, 31400, Toulouse, France*
[c] *CNRS-LMTG, 39 Allées Jules Guesde, 31000, Toulouse, France*

Received 20 December 2002; received in revised form 4 November 2003; accepted 4 December 2003

Abstract

Geochemical and mineralogical data from ancient sedimentary strata can be reliable indicators of the provenance of sediments. The heavy mineral assemblages and the major and trace element contents of sedimentary rocks from the Neogene continental successions of the Central Depression in Chile and the Mauri and Corque Basins in the Altiplano of Bolivia reflect volcanic source rocks with different degrees of magmatic differentiation and alkalinity. These results indicate that the source rocks of the Central Depression were less differentiated (andesite to rhyodacite) than those of the Altiplano basins (rhyodacite to rhyolite). The low concentration (cations per formula unit) of total Al (<0.15 pfu) and [Ca + Na] (~ 0.82 pfu) in the detrital clinopyroxenes and low [Nb/Y] ratio (<0.7) of whole-rock analyses of sandstones from the Central Depression indicate erosion of a calc-alkaline source rock. By contrast, the high concentration of total Al (>0.15 pfu) and [Ca + Na] (~ 0.92 pfu), the variable Ti content (0.01–0.04 pfu) of the clinopyroxenes and the high [Nb/Y] (>0.7) in whole-rock analyses of sandstones from the Mauri Basin indicate erosion of alkaline rock sources. Locally, the low concentration of total Al (<0.15 pfu) in the detrital clinopyroxenes of sandstones from the Corque Basin indicates erosion of a subalkaline source rock. The chemical trends in the sandstones are similar to those in volcanic suites from the Western Cordillera and Eastern Cordillera of the Central Andes.

Keywords: Source rock; Clinopyroxene; Geochemistry; Neogene; Central Depression; Altiplano

1. Introduction

The geochemical characteristics of volcaniclastic sedimentary rocks may be directly related to their source (e.g., Bhatia, 1983; Bhatia and Crook, 1986; Roser and Korsch, 1986). For instance, several geochemical diagrams have been devised to identify the original magmatic affinities of metabasites, based on the assumption that the concentrations of some elements (e.g., Ti, Y, Nb, Zr, Ta) remain constant during the alteration processes (Floyd and Winchester, 1975; Pearce and Norry, 1979). However, transport mecha-

* Corresponding author. Fax: +56-2-6963050.
E-mail address: lpinto@cec.uchile.cl (L. Pinto).

0037-0738/$ - see front matter © 2004 Elsevier B.V. All rights reserved.
doi:10.1016/j.sedgeo.2003.12.002

nisms and mixing of materials from diverse source areas may obscure the original signatures and thus prevent reconstruction of the paleogeography from geochemical analyses (Morton, 1991).

Different combinations of common volcanic minerals may result in similar chemical compositions, and whole-rock chemical analyses can rarely be used to infer the mineralogy of volcaniclastic sediments (Argast and Donnelly, 1987). However, in igneous rock suites it is possible to use chemical variations. For instance, the composition of derivate melts can be inferred from the separation of minerals with known compositional variations. Thus, geochemical analyses of individual detrital mineral grains can be used to infer source rocks (Cawood, 1983, 1991a; Morris, 1988; Krawinkel et al., 1999). Clinopyroxene composition, for example, is a reliable indicator of petrogenetic relationships between arc-derived sandstones (e.g., Cawood, 1983, 1991b; Morris, 1988).

The aim of this paper is to determine the mineralogical and geochemical compositions of the volcaniclastic sedimentary rocks deposited in the Neogene Andean basins of the Central Depression and Altiplano. These data are used to establish the paleogeographic significance of these deposits, as well as the geotectonic environment prevailing during the formation and exposure of the source rocks in the northern segment of the Bolivian orocline during Andean uplift.

No geochemical data for detrital clasts from the studied sedimentary deposits are available. However, geochemical data for whole-rock and individual igneous minerals have been published for samples from the Precordillera, Western Cordillera and Eastern Cordillera (e.g., Soler and Jiménez, 1993; Geobol, 1995; Fornari et al., 1993, 1996; Legros, 1998; García, 2001). These data correspond to the potential sources of the sedimentary rocks we have studied, and therefore can be compared with the geochemical and mineralogical data reported in this paper.

The geochemical data represent a whole-rock signature for the sedimentary rocks, the heavy mineral fraction comprising only a very small part of the rock. However, this fraction offers a more reliable qualitative indication of the source rock composition.

Heavy minerals (HM) from the Central Depression and Altiplano basins (Table 1) permit the identification of four different sources for these sedimentary deposits: (1) volcanic (clinopyroxene, orthopyroxene, amphibole, biotite, titanite, apatite), (2) metamorphic (Fe^{2+} and Mg-rich garnet, staurolite, muscovite, chlorite, epidote, corundum), (3) hydrothermal (tourmaline, pyrite) and (4) pegmatitic (zircon, tourmaline, Mn-rich garnet). Because of the ability of the volcanic rocks to indicate the prevailing tectonic environment, we only consider the volcanic assemblage, specifically the composition of clinopyroxenes, and the whole-rock geochemistry.

2. Geological setting

Along the western margin of South America, the Central Andes (13–24°S) include a major deflection know as the Bolivian orocline (Isacks, 1988) whose axis is identified as the Arica-Santa Cruz bend (Fig. 1). In this region, the Andean chain forms a plateau 3800 m high. The trend of the Andes north of the Arica-Santa Cruz bend is NW–SE, whereas to the south, its orientation is N–S (Fig. 1). Recent work has demonstrated that the eastern flank of the northern branch of the orocline has undergone greater erosion than the southern branch (Masek et al., 1994). In the Central Depression, in Chile, and the Corque and Mauri Basins, in Bolivia (Fig. 2), the thicknesses of the Neogene strata are ~1000 and ~10,000 m, respectively. In addition, extensive Neogene volcanic deposits covering the Western Cordillera between the Altiplano and the Precordillera make it difficult to observe the pre-Neogene erosion surfaces in order to deduce the degree of denudation in this region. Nevertheless, the strata preserved in the Central Depression suggest an intense erosion for this period (Salas et al., 1966; García, 2001). Establishing the erosional history of these morphostructural units would provide clues to understanding the Neogene paleo-relief and the geodynamic evolution of this part of the Central Andes.

3. Stratigraphy

3.1. Central Depression

The Central Depression in Northern Chile (18° 30′ S–24°S) (Fig. 1) corresponds since the Oligocene

Table 1
Concentration of minerals (%) from the heavy fraction of the studied sediments

	Central Depression																		
Fm.	Azapa Fm.						Latagualla Fm.												
Sample	A1	A2	A7	A8	A18	A20	L2	S8	A10	M12	A9	S2	S3	N2	N3	N5	P10	N8	M8
Vol.	x	x	x	x	x	x	x	x	x	x	x	x	x	x	x	x	x	x	x
Met.	x	x	x	x	x	x													
Peg.			x		x	x													
Hyd.	x		x			x													
Grt	3	3	tr	1	1	2							tr		tr				
St		tr																	
Ttn			0.5	0.4		tr			tr				tr						
Ol								tr		5	3	5	tr						10
Zrn			tr			tr													
Cpx		18	tr	18			51	45	73	61	5	71	39	6	17	49	33	37	32
Opx			tr	0.6		tr	47	53	12	26	36	25	59	3	14	41	35	41	59
Amp	tr	19	45	24	tr	tr	1.8	0.6	1		tr		tr	24	58	2	14	2	tr
Bt		8	4	tr			tr	0.6	tr	3	tr	tr	tr	5	2	5	8	8	tr
Ms																			
Chl	tr	tr	tr		tr	tr													
Ep	59	24	40	50	32	12		0.6	0.9	0.1	0.2					tr			
Tur	tr		6			tr													
Crn						tr													
Oxf	38	28	4	6	67	86		0.6	13	5	11	tr	2	8	8	3	10	12	
Py			tr																
Ap			tr		tr				tr										

				Altiplano (Mauri Basin)				Altiplano (Corque Basin)							
Fm.	El Diablo Fm.			Ber. Fm.	Mauri 1–5 Fm.			Coniri Fm.		Caquiav. Fm.		Pomata Fm.		Mauri 6 Fm.	
Sample	A4	A5	A17	B32	B33	B34	B63	B49	B50	B56	B57	B58	B60	B61	B62
Vol.	x	x	x	x	x	x	x	x	x	x	x	x	x	x	x
Met.				x				x	x	x	x				
Peg.			x	x		x	x	x		x					
Hyd.				x				x		x					
Grt				tr		tr	tr	1	1	5	0.5	1	2		tr
St								0.3							
Ttn	1.6		7			7	tr	0.5	5	40	25	16	44	7	15
Ol		1													
Zrn			tr			tr		tr							
Cpx	17	52	tr	10	44	7	80	tr	2	5	3	44	1		1
Opx	26	37													
Amp	22		5		11	77	10		32	20	60	33	39	75	66
Bt	1					2	tr		7		2	tr	tr	15	15
Ms								21	11	8	2				
Chl															
Ep															
Tur				1.3				2	tr	tr	tr				
Crn															
Oxf	33	1	88	89	44	7	10	75	42	16	4	5	10		tr
Py															
Ap				tr		1		tr		5	3	tr	5	3	3

Amp: amphibole, Ap: apatite, Bt: biotite, Chl: chlorite, Cpx: clinopyroxene, Crn: corundum, Ep: epidote, Grt: garnet, Ms: muscovite, Ol: olivine, Opx: orthopyroxene, Oxf: Fe–Ti oxides, Py: pyrite, St: staurolite, Ttn: titanite, Tur: tourmaline, Zrn: zircon; tr (< 0.05%). Size fraction analysed was 0.25–0.5 mm. Identification of minerals was under a binocular lens and verified by petrographic procedures, X-ray diffractometry and microprobe analysis. Volcanic (vol.), metamorphic (met.), pegmatite (peg.) and hydrothermal (hyd.) assemblages for each sample are indicated.

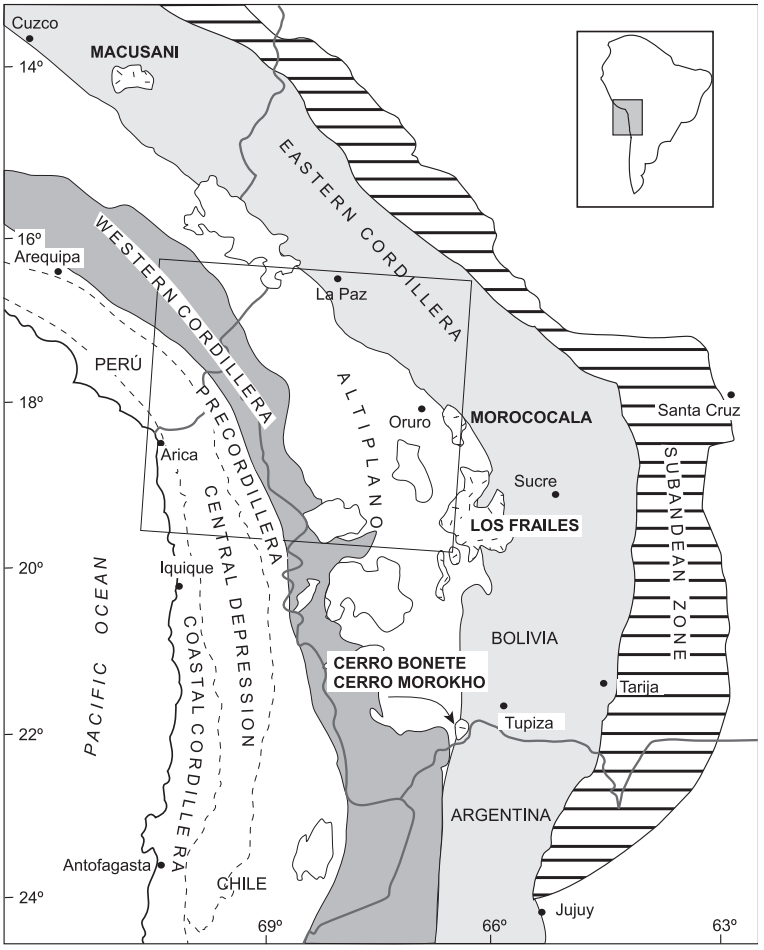

Fig. 1. Morphostructural units in the orocline of the Central Andes. The location of Fig. 2 is indicated.

to a N–S-oriented forearc sedimentary basin. It is bounded to the west by the Coastal Cordillera and to the east by the Precordillera or western slope of the Altiplano. The Precordillera is characterized by the existence of a major system of west-vergent thrust-faults hundreds of kilometers long (Muñoz and Charrier, 1996; García et al., 1999) and flexures (i.e., the Moquella Flexure; Pinto, 1999; Farías et al., 2002).

We have studied the Azapa (Salas et al., 1966), Latagualla (Pinto et al., in press) and El Diablo (Tobar et al., 1968) Formations in the northern Central Depression (Fig. 2), which accumulated during the Late Oligocene–Early Miocene (~ 30–8 Ma; Naranjo and Paskoff, 1985; García, 2001) and are composed of fluvial and alluvial fan conglomerates and coarse sandstones with a few evaporitic horizons, and ignimbrite intercalations (Fig. 2). The conglomerates of the Azapa Formation are polygenetic with volcanic, plutonic and metamorphic clasts. The gravel deposits of the El Diablo Formation are composed of ignimbritic (pumice, quartz, ash), andesitic and basaltic–andesitic fragments. Andesitic fragments are more abundant toward the top of the succession. The sand deposits are composed mainly of volcanic lithics (García, 2001).

3.2. Mauri and Corque Basins

The Altiplano constitutes an extensive intramontane detrital sedimentary basin developed during the Eo-

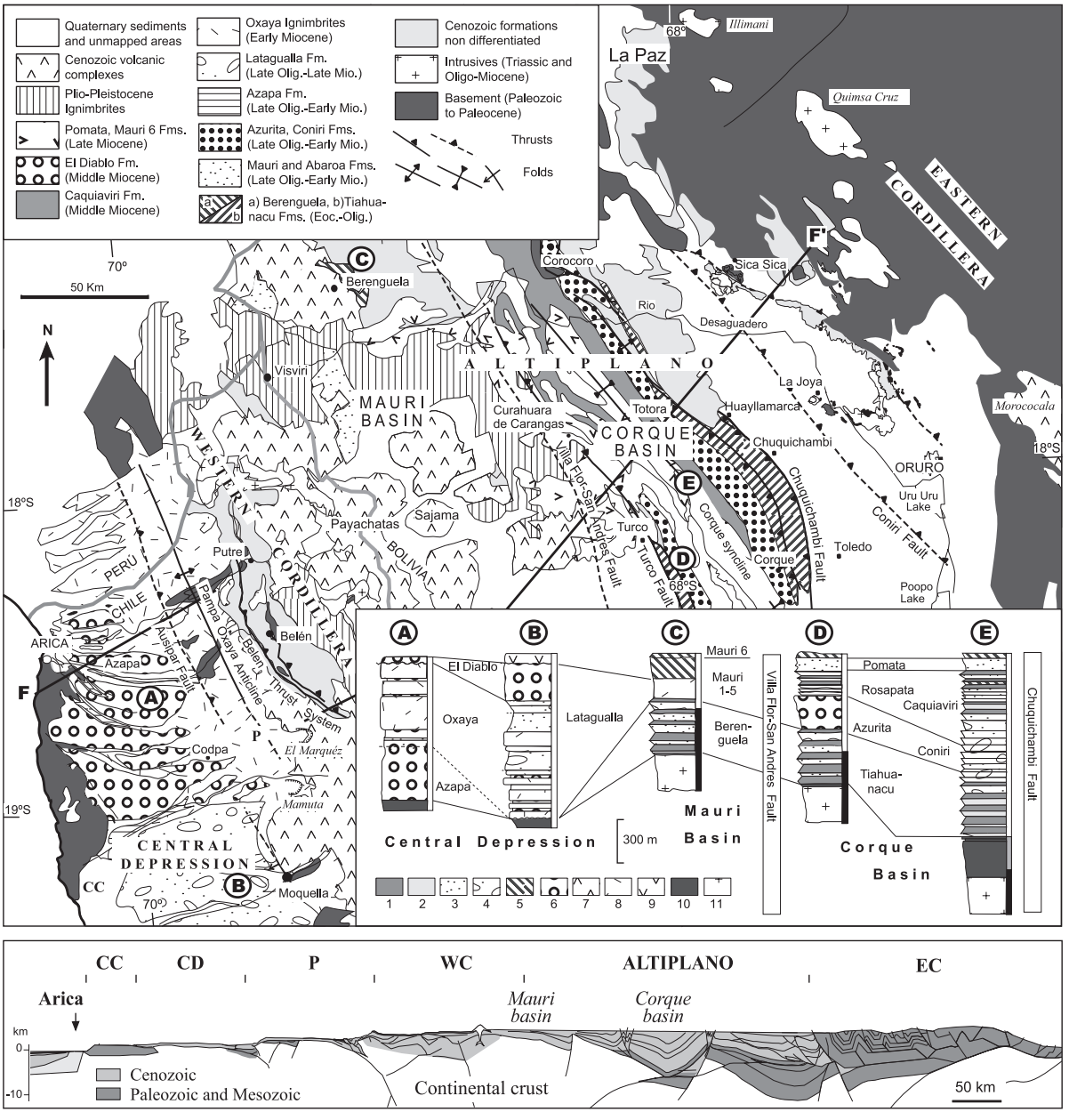

Fig. 2. Generalized geologic map and SW–NE profile of northern Chile and northwestern Bolivia (modified from Hérail et al., in preparation). Stratigraphic symbols: (1) shales; (2) siltstones; (3) sandstones; (4) siltstones, sandstones and conglomerates; (5) conglomerates and greywackes; (6) conglomerates; (7) evaporites; (8) ignimbrites; (9) andesites; (10) Paleozoic and Mesozoic rocks; (11) Precambrian gneiss and granites. CC: Coastal Cordillera, CD: Central Depression, P: Precordillera, WC: Western Cordillera, EC: Eastern Cordillera. F–F′ approximately indicates orientation of the profile.

cene–Pliocene. Geographically, it is bounded to the west by the Western Cordillera, which corresponds to the present day volcanic arc, and to the east by the Eastern Cordillera (Figs. 1 and 2). The Altiplano is structurally delimited in the east by the Huarina Fold and Thrust Belt (Sempere et al., 1988). In the Altiplano, there are two major Neogene basins, the Mauri and the Corque Basins, separated by the east-vergent Villa Flor – San Andrés Faults (Fig. 2) (e.g., Sempere et al., 1988; Hérail et al., 1997; Rochat et al., 1998; Lamb et al., 1997). The Mauri Basin is an eastward-dipping half-graben, whereas the Corque Basin is a wide and deep syncline (10,000 m) (Rochat et al., 1998).

Units studied from the Mauri Basin, in the area of Berenguela, are the Eocene to Pliocene Berenguela and Mauri 1–6 Formations (Lavenu et al., 1989; Marshall et al., 1992; Montes de Oca et al., 1963; Sirvas and Torres, 1966) (Fig. 2). The Berenguela Formation is composed mainly of coarse quartzitic sandstones, with conglomerate and shale intercalations, deposited in alluvial fans. The conglomerate intercalations contain abundant red granite and granulitic gneiss clasts (Rochat, 2002). The Mauri 1–6 Formation consists of volcaniclastic conglomerates and sandstones, basaltic lavas and ignimbrites (Lavenu et al., 1989; Geobol, 1995; Rochat, 2002). The igneous rocks of the Mauri Formation are alkaline near the base, becoming calc-alkaline towards the top (Geobol, 1995).

The units studied in the Corque Basin of the Chuquichambi-Turco region (Fig. 2) are the Late Oligocene to Pliocene Coniri, Caquiaviri, Pomata and Mauri 6 Formations (Ahlfeld, 1946; Sirvas and Torres, 1966; Ascarrunz et al., 1967; Rochat et al., 1998; Rochat, 2002). In the center of the basin, the Coniri, Caquiaviri, Pomata and Mauri 6 Formations consist of alluvial fan and fluvial coarse sandstones and conglomerates. The Coniri Formation contains granitic and sedimentary clasts, whereas the Caquiaviri and Pomata Formations contain sedimentary, granitic and volcanic clasts. The volcaniclastic sedimentary deposits of the Mauri 6 Formation are mainly reworked tuffs (Rochat, 2002).

4. Analytical procedures

The volcaniclastic successions were sampled from seven localities indicated in Fig. 3. We analyzed 38 semi-consolidated sandstone samples selected from medium-grained sandstones and taken at equal distances in order to represent the complete stratigraphic sequence.

The separation and preparation of heavy minerals followed procedures described by Parfenoff et al. (1970) and Mange and Maurer (1991). Each sample was disaggregated and the heavy minerals concentrated using a wash pan. The 0.25–0.50 mm fraction was obtained by sieving, the heavy mineral fraction was separated with bromoform ($d = 2.9$), and 200 grains from each sample were point-counted as described by Mange and Maurer (1991). As samples A26, C1, S1 and A24 were too difficult to disaggregate they were not analyzed for their heavy mineral content.

For preparation, individual grains were hand picked, mounted in epoxy, ground, polished and coated with carbon. Mineral analyses were carried out at the Equipe de Minéralogie, Laboratoire de Mécanismes de Transfert en Géologie (CNRS-IRD-Université Paul Sabatier, Toulouse). Heavy minerals were identified using standard mineralogical procedures, X-ray diffractometry (Debye-Scherrer Method, 57.3 mm of diameter, radiation $K_{\alpha}Cu$) and chemical analysis (Table 1). The chemical composition of 297 optically homogeneous single clinopyroxenes of 30 representative samples was determined using an electron microprobe SX-50 CAMEBAX (182 clinopyroxenes from the Central Depression samples and 115 from the Altiplano). At least five clinopyroxene grains were analyzed in each sample. The electron microprobe analyses were carried out for SiO_2, TiO_2, Al_2O_3, Cr_2O_3, FeO, MnO, MgO, CaO, Na_2O and K_2O. The structural formulae of pyroxenes were calculated on the basis of four cations, the respective amounts of Fe^{3+} and Fe^{2+} being calculated on the basis of six oxygens, Cr being taken as Cr^{3+} and Ti as Ti^{4+} (Table 2).

Major element analyses of whole-rocks (Table 3) were carried out by ICP-AES at the Service d'Analyse des Roches et des Minéraux (Centre de Recherches Pétrographiques et Géochimiques, Vandoeuvre-lés-Nancy, France). Trace element analyses of whole-rocks (Table 3) were done by ICP-MS in the Equipe de Géochimie of the Laboratoire de Mécanismes de Transfert en Géologie (CNRS-IRD-Université Paul Sabatier, Toulouse).

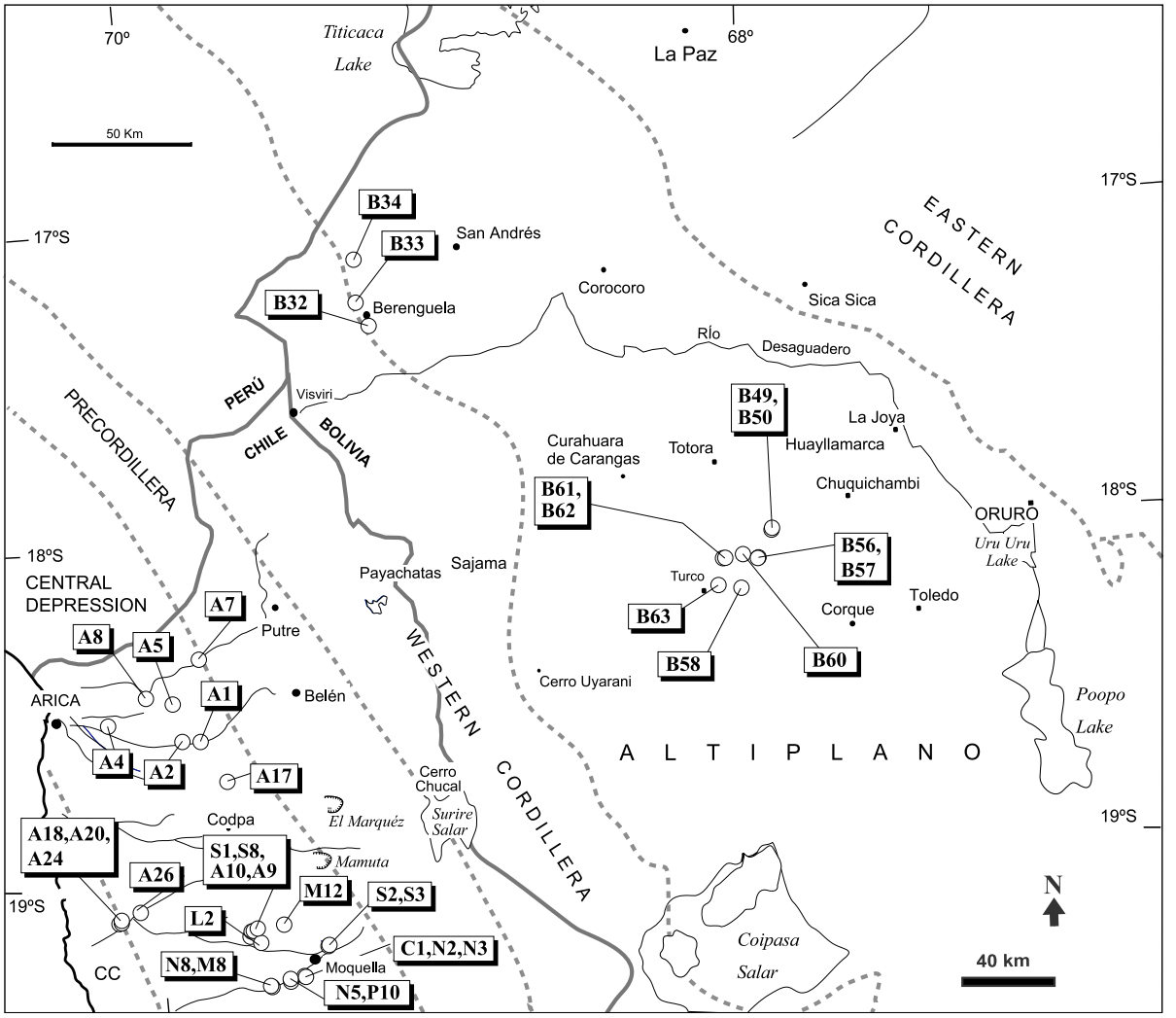

Fig. 3. Sample distribution in the Neogene sedimentary basins. CC: Coastal Cordillera.

Analyses of X-ray diffraction (XRD) were made on some samples of the matrix of the sandstones. These were obtained by sieving out the >63-μm fraction, after which the silt and clay were separated by decantation using Stokes' Law. The fractions obtained were dried in an oven below 30 °C. Diffractograms were run at the Equipe de Minéralogie of the Laboratoire de Mécanismes de Transfert en Géologie (CNRS-IRD-Université Paul Sabatier, Toulouse) and at the Servicio Nacional de Geología y Minería (SERNAGEOMIN, Santiago, Chile).

5. Sediment composition

The heavy minerals are not altered and possess a great internal homogeneity shown by the compositional homogeneity of profiles through the same mineral grain. The sedimentary rocks have undergone little alteration due to the semi-arid climate existing in the region during the Neogene (e.g., Alpers and Brimhall, 1988). In addition, structural studies indicate that sedimentation was very fast near the deformation areas, protecting them from alteration. On the

Table 2
Chemical analyses of representative detrital clinopyroxenes from the Neogene sedimentary rocks of the Central Depression and Altiplano basins

	Central Depression															
Fm.	Azapa Fm.			Latagualla Fm.												
Sample	A7	A8	A2	L2	S8	A10	M12	S2	S3	A9	N2	N3	N5	P10	M8	N8
Code	A7IIb 9	A8IIb 6	A2IIa 15	L2IVa 18	S8IVa 21	A10IVa 1	M12IVa 21	S2IVa 7	S3IVa 18	A9IVa 31	N2IVa 20	N3IVa 5	N5IVa 3	P10IVa 13	M8IVa 11	N8IVa 6
SiO_2	52.25	51.12	52.58	52.16	52.67	51.59	52.39	52.00	51.71	51.50	51.11	52.58	52.59	52.23	51.98	52.13
TiO_2	0.22	0.65	0.18	0.39	0.45	0.58	0.54	0.48	0.64	0.44	0.60	0.43	0.38	0.39	0.49	0.52
Al_2O_3	1.76	2.96	1.68	1.43	1.46	1.64	1.35	1.32	1.68	1.35	3.19	2.02	1.54	1.22	1.37	1.40
Cr_2O_3	0.34	0.07	0.17	0.02	0.10	0.04	0.01	0.00	0.08	0.00	0.00	0.00	0.01	0.05	0.03	0.00
Fe_2O_3(c)	3.57	1.88	3.61	1.45	0.08	2.41	0.47	1.95	1.78	3.16	2.36	1.03	0.77	1.77	1.40	1.73
FeO(c)	2.89	7.78	2.70	9.63	10.43	8.28	11.40	8.78	9.29	8.22	6.83	8.22	8.94	8.57	10.67	9.78
MnO	0.14	0.22	0.17	0.25	0.23	0.36	0.31	0.24	0.25	0.25	0.26	0.31	0.28	0.31	0.25	0.39
MgO	17.67	14.83	17.76	14.44	14.42	14.49	14.54	14.50	14.65	14.34	14.56	15.52	14.66	14.49	14.35	14.70
CaO	20.96	20.14	20.69	19.85	20.04	20.19	18.72	20.32	19.63	20.29	20.74	19.70	20.44	20.62	19.32	19.44
Na_2O	0.28	0.31	0.42	0.36	0.29	0.39	0.33	0.37	0.35	0.42	0.44	0.38	0.36	0.36	0.29	0.32
K_2O	0.00	0.00	0.02	0.00	0.00	0.03	0.00	0.00	0.00	0.00	0.00	0.03	0.00	0.00	0.00	0.01
Total	100.09	99.98	99.99	99.98	100.17	99.98	100.05	99.96	100.06	99.97	100.1	100.22	99.98	100.01	100.14	100.41
Numbers of ions on the basis of 6 O																
Si	1.91	1.90	1.92	1.95	1.96	1.93	1.96	1.94	1.93	1.93	1.90	1.94	1.96	1.95	1.95	1.94
Al/Al^{IV}	0.08	0.10	0.07	0.05	0.04	0.07	0.04	0.06	0.07	0.06	0.10	0.06	0.04	0.05	0.05	0.06
Al^{VI}	0.00	0.03	0.00	0.01	0.03	0.00	0.02	0.00	0.01	0.00	0.04	0.03	0.03	0.00	0.01	0.00
Ti	0.01	0.02	0.01	0.01	0.01	0.02	0.02	0.01	0.02	0.01	0.02	0.01	0.01	0.01	0.01	0.02
Cr	0.01	0.00	0.01	0.00	0.00	0.00	0.00	0.00	0.00	0.00	0.00	0.00	0.00	0.00	0.00	0.00
Fe^{3+}	0.10	0.05	0.10	0.04	0.00	0.07	0.01	0.06	0.05	0.09	0.07	0.03	0.02	0.05	0.04	0.05
Fe^{2+}	0.09	0.24	0.08	0.30	0.33	0.26	0.36	0.27	0.29	0.26	0.21	0.25	0.28	0.27	0.33	0.31
Mn^{2+}	0.00	0.01	0.01	0.01	0.01	0.01	0.01	0.01	0.01	0.01	0.01	0.01	0.01	0.01	0.01	0.01
Mg	0.96	0.82	0.97	0.81	0.80	0.81	0.81	0.81	0.82	0.80	0.81	0.86	0.81	0.81	0.80	0.82
Ca	0.82	0.80	0.81	0.80	0.80	0.81	0.75	0.81	0.79	0.81	0.83	0.78	0.82	0.83	0.78	0.78
Na	0.02	0.02	0.03	0.03	0.02	0.03	0.02	0.03	0.03	0.03	0.03	0.03	0.03	0.03	0.02	0.02
K	0.00	0.00	0.00	0.00	0.00	0.00	0.00	0.00	0.00	0.00	0.00	0.00	0.00	0.00	0.00	0.00
Cat#	4.00	4.00	4.00	4.00	4.00	4.00	4.00	4.00	4.00	4.00	4.00	4.00	4.00	4.00	4.00	4.00
Atomic percentages																
Wo	41.62	41.67	41.12	40.82	41.24	41.33	38.66	41.33	40.31	41.12	43.01	40.41	42.27	42.13	39.80	39.59
En	48.73	42.71	49.24	41.33	41.24	41.33	41.75	41.33	41.84	40.61	41.97	44.56	41.75	41.12	40.82	41.62
Fs[a]	9.64	15.63	9.64	17.86	17.53	17.35	19.59	17.35	17.86	18.27	15.03	15.03	15.98	16.75	19.39	18.78
X_{Mg}[b]	0.92	0.77	0.92	0.73	0.71	0.76	0.69	0.75	0.74	0.76	0.79	0.77	0.75	0.75	0.71	0.73

[a] $Fs=(Fe^{2+}+Fe^{3+}+Mn^{2+})/(Fe^{2+}+Fe^{3+}+Mn^{2+}+Mg+Ca)$.

[b] $X_{Mg}=Fe^{2+}/(Fe^{2+}+Mg)$.

	Central Depression			Altipano (Mauri Basin)				Altiplano (Corque Basin)							
Fm.	El Diablo Fm.			Ber. Fm.	Mauri Fm.			Coniri Fm.		Caquiaviri Fm.		Pomata Fm.		Mauri 6 Fm.	
Sample	A4	A5	A17	B32	B33	B34	B63	B49	B50	B56	B57	B58	B60	B61	B62
Code	A4IVa 2	A5a 3	A17IIb 18	B32 16	B33 13	B34 4	B63 3	B49 50	B50 14	B56 27	B57 27	B58 14	B60 22	B61 14	B62 40
SiO_2	52.19	51.16	52.43	47.18	48.73	50.90	47.36	54.43	47.89	52.5	53.12	50.58	52.64	53.21	52.81
TiO_2	0.19	0.56	0.15	1.01	1.13	0.48	1.47	0.06	1.39	0.14	0.13	1.14	0.11	0.14	0.05
Al_2O_3	1.02	1.51	0.83	6.11	4.71	3.62	6.60	1.03	4.75	0.93	0.74	2.76	0.85	0.40	0.70
Cr_2O_3	0.00	0.05	0.00	0.04	0.00	0.52	0.01	0.75	0.08	0.04	0.00	0.04	0.04	0.02	0.00
Fe_2O_3(c)	2.38	1.61	2.15	6.46	4.71	2.61	3.56	0.17	4.44	2.65	1.51	1.78	1.56	1.58	2.15
FeO(c)	7.98	11.33	7.31	1.79	4.12	3.15	4.70	2.89	5.37	6.36	6.94	6.96	7.02	8.09	7.17
MnO	0.36	0.37	0.43	0.21	0.22	0.07	0.17	0.06	0.26	0.33	0.46	0.28	0.41	0.50	0.48
MgO	14.30	13.59	14.60	13.59	13.85	15.32	12.69	17.78	12.94	13.44	13.64	13.89	13.44	13.63	13.06
CaO	21.28	19.16	21.52	22.74	22.35	23.13	22.18	22.96	21.92	23.02	23.10	21.95	23.09	22.33	22.96
Na_2O	0.32	0.26	0.31	0.42	0.34	0.24	0.44	0.23	0.37	0.59	0.50	0.30	0.44	0.48	0.62
K_2O	0.00	0.00	0.02	0.01	0.01	0.00	0.00	0.00	0.00	0.01	0.00	0.00	0.02	0.00	0.00
Total	100.01	99.59	99.76	99.56	100.18	100.05	99.18	100.36	99.41	100.01	100.14	99.69	99.61	100.39	100.00
Numbers of ions on the basis of 6 O															
Si	1.95	1.94	1.96	1.76	1.81	1.87	1.78	1.97	1.81	1.96	1.98	1.89	1.97	1.98	1.98
Al/Al^{IV}	0.05	0.06	0.04	0.24	0.19	0.13	0.22	0.03	0.20	0.04	0.02	0.11	0.03	0.02	0.03
Al^{VI}	0.00	0.00	0.00	0.03	0.02	0.03	0.07	0.02	0.02	0.00	0.01	0.01	0.01	0.00	0.01
Ti	0.01	0.02	0.00	0.03	0.03	0.01	0.04	0.00	0.04	0.00	0.00	0.03	0.00	0.00	0.00
Cr	0.00	0.00	0.00	0.00	0.00	0.02	0.00	0.02	0.00	0.00	0.00	0.00	0.00	0.00	0.00
Fe^{3+}	0.07	0.05	0.06	0.18	0.13	0.07	0.10	0.01	0.13	0.07	0.04	0.05	0.04	0.04	0.06
Fe^{2+}	0.25	0.36	0.23	0.06	0.13	0.10	0.15	0.09	0.17	0.20	0.22	0.22	0.22	0.25	0.22
Mn^{2+}	0.01	0.01	0.01	0.01	0.01	0.00	0.01	0.00	0.01	0.01	0.02	0.01	0.01	0.02	0.02
Mg	0.80	0.77	0.81	0.76	0.77	0.84	0.71	0.96	0.73	0.75	0.76	0.78	0.75	0.76	0.73
Ca	0.85	0.78	0.86	0.91	0.89	0.91	0.89	0.89	0.89	0.92	0.92	0.88	0.93	0.89	0.92
Na	0.02	0.02	0.02	0.03	0.02	0.02	0.03	0.02	0.03	0.04	0.04	0.02	0.03	0.04	0.05
K	0.00	0.00	0.00	0.00	0.00	0.00	0.00	0.00	0.00	0.00	0.00	0.00	0.00	0.00	0.00
Cat#	4.00	4.00	4.00	4.00	4.00	4.00	4.00	4.00	4.00	4.00	4.00	4.00	4.00	4.00	4.00
Atomic percentages															
Wo	42.93	39.59	43.65	39.56	39.88	43.71	38.27	49.33	37.96	38.29	38.80	40.11	38.38	38.62	37.37
En	40.40	39.09	41.12	47.62	46.26	47.40	48.09	45.79	46.21	47.21	47.21	45.55	47.44	45.46	47.23
Fs[a]	16.67	21.32	15.23	12.82	13.86	8.89	13.64	4.88	15.82	14.51	13.99	14.34	14.18	15.92	15.40
X_{Mg}[b]	0.76	0.68	0.78	0.93	0.86	0.90	0.83	0.92	0.81	0.79	0.78	0.78	0.77	0.75	0.76

Table 3
Major element and trace element concentrations of the whole-rock of studied sedimentary rocks

Fm. sample	Central Depression											
	Azapa Fm.							Latagualla Fm.				
	A26	A1	A2	A7	A8	A18	A20	C1	L2	S1	S8	A10
Major elements (wt.%)												
SiO_2	61.67	53.79	56.59	61.05	55.81	69.6	68.78	62.46	57.84	53.57	60.04	59.87
Al_2O_3	12.24	13.53	12.82	14.67	15.62	12.9	12.84	14.55	15.28	14.12	15.60	14.25
Fe_2O_3	3.45	6.36	5.63	5.28	7.00	3.68	4.88	4.88	6.45	5.97	6.02	5.77
MnO	0.06	0.10	0.08	0.10	0.06	0.05	0.06	0.07	0.10	0.06	0.08	0.08
MgO	1.25	2.51	2.51	2.28	2.82	1.23	1.16	1.27	5.07	3.21	3.36	2.11
CaO	5.99	8.27	7.00	4.09	5.45	1.81	1.62	4.40	6.10	6.28	4.79	4.37
Na_2O	2.79	2.04	2.11	2.80	2.63	2.50	2.86	2.74	2.79	3.28	3.23	3.20
K_2O	2.94	2.01	2.39	3.08	2.52	3.11	3.11	2.71	1.94	2.60	2.53	2.87
TiO_2	0.43	0.69	0.66	0.66	0.78	0.48	0.62	0.55	0.65	0.66	0.72	0.69
P_2O_5	0.12	0.16	0.18	0.16	0.18	0.12	0.13	0.15	0.14	0.17	0.13	0.13
IL[a]	8.94	10.47	9.94	6.14	7.00	4.38	3.79	6.12	3.53	10.57	3.38	6.54
IM[b]	5.04	3.98	4.41	4.16	3.57	5.40	5.36	4.29	3.79	3.79	3.85	4.20
Na_2O/K_2O	0,95	1,01	0,88	0,91	1,04	0,80	0,92	1,01	1,44	1,26	1,28	1,11
CIA[c]	0.51	0.52	0.53	0.60	0.60	0.63	0.63	0.60	0.59	0.54	0.60	0.58
AI[d]	1.81	2.21	1.95	1.92	2.36	1.24	1.36	1.65	1.87	3.27	1.99	2.12
Trace elements (ppm)												
Cs	5.36	7.36	5.55	29.17	2.61	3.88	3.70	7.72	5.11	5.19	5.82	7.01
Rb	98.41	77.49	88.21	142.82	99.03	100.24	98.99	75.85	103.63	121.39	118.76	125.58
U	2.17	1.85	2.26	2.14	1.69	2.52	2.29	1.45	4.07	4.52	4.59	5.45
Th	8.92	7.17	7.56	9.55	7.80	9.37	9.77	7.79	15.85	13.19	18.48	16.57
Sr	451.84	708.57	725.11	457.01	477.56	211.41	227.75	596.29	392.28	386.93	455.9	470.21
Ba	707.27	655.14	702.84	659.39	488.23	677.56	665.51	630.13	461.32	562.77	668.03	735.91
La	21.12	25.03	23.99	24.19	25.07	21.15	22.34	27.56	23.63	22.91	28.09	25.16
Ce	39.93	50.01	47.34	49.62	49.70	42.37	43.91	48.88	50.57	38.37	57.04	51.76
Ta	0.73	0.87	0.78	0.71	0.74	1.04	0.79	0.61	0.73	0.63	0.82	1.07
Nb	7.14	8.15	9.31	8.57	7.92	8.22	8.93	8.24	7.76	7.27	9.65	10.10
Hf	3.71	3.70	4.16	4.67	4.59	3.55	3.98	3.92	5.00	4.12	5.68	5.41
Nd	18.64	24.40	23.19	23.43	22.84	18.89	19.23	20.50	21.48	19.54	24.88	23.47
Zr	143.51	155.30	167.46	183.98	189.08	134.58	153.71	154.71	192.01	157.65	216.78	209.8
Sm	3.66	5.06	4.73	4.55	4.29	3.70	3.75	3.65	4.18	3.67	4.58	4.40
Eu	0.78	1.17	1.06	1.04	1.10	0.81	0.79	0.88	0.81	0.79	1.00	0.80
Yb	1.85	2.31	2.09	2.10	1.87	1.86	1.97	1.55	1.63	1.49	1.77	1.73
Y	16.62	23.44	21.26	20.88	19.23	17.14	17.99	16.28	17.59	16.22	19.01	17.23
V	79.42	148.60	134.11	127.55	192.98	85.15	108.49	88.63	132.19	139.25	131.32	135.66
Co	7.47	13.19	11.86	13.08	17.86	7.21	8.23	10.19	25.70	19.73	19.94	17.56
Cr	6.21	32.78	35.28	21.88	36.96	12.96	15.47	4.68	167.49	65.52	67.50	50.44
Ni	10.87	20.23	23.30	15.40	18.33	12.56	11.47	5.51	74.68	29.92	34.25	27.55
Nb/Y	0.43	0.35	0.44	0.41	0.41	0.48	0.50	0.51	0.44	0.45	0.51	0.59
Zr/Ti[e]	0.03	0.02	0.03	0.03	0.02	0.03	0.02	0.03	0.03	0.02	0.03	0.03
La/Yb	11.42	10.84	11.46	11.50	13.43	11.39	11.32	17.73	14.46	15.41	15.86	14.51

Major element analyses of whole-rocks were carried out by ICP-AES and trace element analyses of whole-rocks by ICP-MS.

[a] IL: ignition loss.

[b] IM (maturity index) = SiO_2/Al_2O_3.

[c] CIA = $Al_2O_3/(Al_2O_3 + CaO + Na_2O + K_2O)$ (after Nesbitt and Young, 1982).

[d] AI (alkalinity index)=$(Na_2O + K_2O)/((SiO_2 - 43)*0.17)$ (after Middlemost, 1975).

[e] Zr/Ti=$(Zr*10{,}000/TiO_2)$.

										El Diablo Fm.			
M12	A9	S2	S3	N2	N3	N5	P10	N8	M8	A4	A5	A17	A24
61.48	59.43	59.27	59.02	50.51	55.67	61.13	59.87	58.66	57.5	64.92	54.84	60.87	55.53
14.87	17.17	15.53	15.81	16.9	19.3	15.42	17.85	16.61	15.68	14.38	14.44	14.94	16.60
6.13	6.13	8.15	6.31	5.98	7.10	6.21	4.91	5.90	7.27	5.04	7.17	8.46	5.32
0.08	0.08	0.11	0.08	0.23	0.05	0.10	0.07	0.08	0.10	0.07	0.10	0.28	0.05
3.55	2.95	3.23	4.19	4.57	1.69	3.27	2.10	3.20	4.70	1.77	3.96	2.14	3.43
4.27	5.50	5.01	5.51	3.85	5.71	4.69	5.52	5.32	5.77	3.27	6.50	3.62	5.53
3.02	3.86	3.38	2.92	1.81	3.70	3.04	3.56	3.24	3.07	4.01	4.48	3.01	2.42
3.15	2.01	2.40	2.60	1.86	1.16	2.97	2.49	2.54	2.42	2.65	2.35	2.29	1.63
0.71	0.69	0.92	0.71	0.63	0.78	0.76	0.57	0.69	0.78	0.52	0.77	0.78	0.65
0.15	0.17	0.24	0.16	0.15	0.26	0.19	0.19	0.15	0.19	0.11	0.16	0.14	0.12
2.48	1.91	1.67	2.59	13.39	4.47	2.71	2.79	3.50	2.41	3.14	5.12	2.17	8.59
4.13	3.46	3.82	3.73	2.99	2.88	3.96	3.35	3.53	3.67	4.51	3.80	4.07	3.35
0,96	1,92	1,41	1,12	0,97	3,19	1,02	1,43	1,28	1,27	1,51	1,91	1,31	1,48
0.59	0.60	0.59	0.59	0.69	0.65	0.59	0.61	0.60	0.58	0.59	0.52	0.63	0.63
1.96	2.10	2.09	2.03	2.87	2.26	1.95	2.11	2.17	2.23	1.79	3.39	1.74	1.90
7.14	2.69	5.84	7.16	15.15	10.43	10.11	13.16	26.53	7.60	3.46	3.32	4.03	5.89
155.67	71.74	79.92	128.18	63.14	30.34	146.74	105.87	123.28	111.67	74.35	85.70	65.11	80.58
5.79	2.23	2.46	4.60	0.84	0.84	4.92	2.84	4.33	3.53	1.64	2.56	1.88	3.13
22.75	8.00	9.66	18.27	5.01	5.12	20.83	11.10	17.13	14.05	8.46	12.01	10.25	19.71
347.87	600.44	516.51	411.76	405.11	638.05	374.23	620.6	507.09	501.12	344.46	468.20	483.34	505.71
578.79	675.65	667.05	579.47	715.14	555.69	620.24	650.89	628.17	546.83	675.18	574.00	976.83	526.53
30.09	20.32	25.00	26.33	24.57	26.03	28.56	23.41	24.63	22.72	24.36	25.88	35.00	24.16
60.13	42.52	49.72	54.95	48.11	51.49	59.64	49.20	51.66	47.73	47.63	53.61	76.55	54.84
0.89	0.62	0.61	0.72	0.50	0.52	0.92	0.58	0.60	2.21	0.72	0.62	1.07	0.82
10.74	6.67	8.50	8.70	6.90	7.96	10.77	7.29	8.19	9.99	7.41	8.62	10.87	8.84
6.07	4.38	4.19	5.39	4.20	4.43	6.85	4.45	5.21	4.60	3.78	4.60	6.12	5.22
26.31	20.43	22.66	23.36	21.64	22.87	25.12	21.63	22.67	22.24	19.46	24.13	34.55	22.67
233.05	165.88	168.80	208.60	162.73	185.29	264.66	170.28	208.24	197.81	148.31	182.39	270.39	205.47
4.78	3.91	4.37	4.31	4.06	4.25	4.60	3.99	4.27	4.18	3.54	4.54	6.34	4.24
0.82	0.96	0.96	0.90	1.04	1.16	1.03	1.04	0.98	0.81	0.89	0.98	1.25	0.92
1.93	1.45	1.66	1.66	1.72	1.62	1.95	1.33	1.57	1.59	1.46	1.79	2.16	1.52
20.27	14.62	18.01	17.97	17.68	16.84	20.03	14.41	17.06	16.79	13.95	18.61	22.75	15.03
140.37	133.97	197.77	133.43	126.85	143.24	128.91	84.41	124.57	173.12	108.8	178.66	260.08	143.70
19.90	18.22	21.75	22.48	16.06	13.35	18.86	12.87	20.01	26.15	13.09	24.74	19.58	16.14
62.83	19.81	28.33	104.12	11.27	15.92	74.03	13.72	61.15	94.74	2.64	52.65	32.68	44.37
37.19	19.41	19.38	53.37	7.77	9.58	30.51	12.91	33.62	50.71	9.80	36.44	47.79	28.98
0.53	0.46	0.47	0.48	0.39	0.47	0.54	0.51	0.48	0.60	0.53	0.46	0.48	0.59
0.03	0.02	0.02	0.03	0.03	0.02	0.03	0.03	0.03	0.03	0.03	0.02	0.03	0.03
15.55	14.06	15.07	15.88	14.27	16.05	14.62	17.62	15.74	14.26	16.65	14.50	16.21	15.89

(continued on next page)

Table 3 (*continued*)

Fm.	Altiplano (Mauri Basin)				Altiplano (Corque Basin)							
sample	Ber. Fm.	Mauri Fm.			Coniri Fm.		Caquiaviri Fm.		Pomata Fm.		Mauri 6 Fm.	
	B32	B33	B34	B63	B49	B50	B56	B57	B58	B60	B61	B62
Major elements (wt.%)												
SiO_2	68.39	65.52	65.15	63.94	91.36	83.03	85.63	87.35	68.42	74.02	68.19	67.99
Al_2O_3	11.12	11.16	15.37	14.29	3.42	6.00	6.17	5.09	13.58	12.84	13.62	15.00
Fe_2O_3	3.23	3.14	4.41	6.18	1.69	2.33	1.93	1.67	1.86	3.18	2.95	3.57
MnO	0.05	0.05	0.06	0.10	0.00	0.03	0.00	0.00	0.09	0.03	0.05	0.05
MgO	0.40	0.45	1.60	1.63	0.32	0.56	0.45	0.47	0.76	0.61	1.18	1.19
CaO	5.35	7.28	3.62	3.77	0.36	1.99	0.84	0.79	2.51	1.37	1.84	2.55
Na_2O	1.49	0.19	3.32	3.31	0.44	0.86	1.08	0.75	3.03	2.78	2.67	3.86
K_2O	2.40	2.61	2.78	3.30	0.83	1.43	1.37	1.16	3.87	3.03	4.87	3.73
TiO_2	0.40	0.39	0.53	0.90	0.20	0.37	0.27	0.21	0.23	0.49	0.48	0.57
P_2O_5	0.09	0.07	0.19	0.34	0.08	0.10	0.06	0.08	0.07	0.05	0.18	0.15
IL[a]	6.96	9.00	2.92	2.19	1.11	3.07	1.86	2.28	5.40	1.93	3.84	1.32
IM[b]	6.15	5.87	4.24	4.47	26.71	13.84	13.88	17.16	5.04	5.76	5.01	4.53
Na_2O/K_2O	0,62	0,07	1,19	1,00	0,53	0,60	0,79	0,65	0,78	0,92	0,55	1,03
CIA[c]	0.55	0.53	0.61	0.58	0.68	0.58	0.65	0.65	0.59	0.64	0.59	0.60
AI[d]	0.90	0.73	1.62	1.86	0.15	0.34	0.34	0.25	1.60	1.10	1.76	1.79
Trace elements (ppm)												
Cs	2.42	9.06	2.33	1.63	1.7	2.78	2.11	2.44	6.26	3.75	5.70	2.01
Rb	81.82	95.95	69.35	77.47	29.43	48.48	38.71	40.02	176.21	100.16	163.67	89.33
U	1.33	1.26	1.36	1.51	0.95	1.60	0.93	1.00	3.78	1.84	4.16	1.70
Th	6.79	5.57	6.48	6.90	3.33	5.91	3.93	3.93	10.26	8.15	15.92	7.59
Sr	197.39	183.78	776.30	555.38	78.58	219.67	336.99	311.62	176.31	428.31	389.61	823.63
Ba	916.38	829.16	1148.40	1124.77	470.80	460.2	504.69	473.98	351.65	981.65	630.79	1281.89
La	22.00	19.43	31.57	47.39	11.51	18.19	15.07	14.07	17.58	29.04	46.27	39.70
Ce	42.75	35.94	59.51	85.77	23.16	37.69	30.39	26.32	35.73	54.92	74.04	74.86
Ta	2.45	2.21	4.04	3.51	1.56	2.37	1.75	1.51	9.96	3.86	4.02	3.84
Nb	8.76	8.80	16.56	23.29	5.68	10.13	7.98	6.34	45.47	20.32	21.85	20.99
Hf	4.41	3.62	3.99	4.32	5.71	7.45	4.78	4.89	3.68	5.26	4.36	4.27
Nd	18.39	16.07	24.49	35.97	10.11	16.77	12.87	11.55	15.67	23.32	25.89	29.19
Zr	175.72	140.59	169.57	215.67	273.07	337.20	225.83	222.60	118.64	235.84	175.87	194.15
Sm	3.51	3.18	4.10	6.15	1.98	3.45	2.35	2.12	3.34	4.10	3.96	4.65
Eu	1.01	0.83	1.22	1.56	0.43	0.50	0.54	0.46	0.64	1.04	0.99	1.20
Yb	1.71	1.74	0.99	1.53	1.12	1.83	1.02	1.03	1.99	1.31	0.80	0.85
Y	15.27	16.23	11.44	18.82	10.70	17.23	9.95	10.23	20.90	13.57	9.15	10.33
V	72.61	75.78	84.69	145.25	28.54	42.12	31.55	29.10	28.84	57.11	48.08	64.15
Co	7.62	8.61	8.80	13.13	3.04	4.70	3.26	2.99	3.67	5.72	6.79	7.34
Cr	8.50	9.15	20.11	22.70	8.05	17.75	8.69	6.29	4.17	13.92	14.56	21.23
Ni	12.13	13.19	9.48	13.8	6.15	9.05	6.25	6.03	5.63	9.08	11.83	12.20
Nb/Y	0.57	0.54	1.45	1.24	0.53	0.59	0.80	0.62	2.18	1.50	2.39	2.03
Zr/Ti[e]	0.04	0.04	0.03	0.02	0.14	0.09	0.08	0.11	0.05	0.05	0.04	0.03
La/Yb	12.87	11.19	31.86	30.89	10.29	9.94	14.82	13.61	8.83	22.19	58.16	46.80

other hand, the shallow burial of the sedimentary deposits prevented their diagenesis.

The heavy mineral assemblages and their composition reflect the overall signature (alkalinity and degree of magmatic differentiation) of the volcanic source rocks. In two analyzed regions, olivine and pyroxenes indicate a mafic igneous source whereas amphiboles, biotite, titanite and apatite suggest an intermediate to felsic igneous source.

Here, we will focus on analysis of the clinopyroxenes, because the character of the mafic source can be accurately determined by them (Cawood, 1983; Kra-

winkel et al., 1999). This analysis of the source rock is complemented by data on the major and trace element composition.

5.1. Pyroxenes

Orthopyroxenes (OPx) and clinopyroxenes (CPx) are the most abundant minerals in the heavy fractions from the sandstones in the Central Depression, with contents reaching 73% and 59%, respectively (Table 1). In contrast, only the CPx are locally abundant (up to 80%) in the heavy fraction from the Altiplano sandstones (Table 1).

CPx from both regions show broad variations in composition, which are expected to be related to the chemistry of their host magmatic rocks (Kushiro, 1960; Le Bas, 1962; Nisbet and Pearce, 1977; Leterrier et al., 1982; Deer et al., 1978; Cameron and Papike, 1981). For instance, CPx from alkali basalts are enriched in Al, Na and Ti, and depleted in Si compared to CPx from other types of basalts.

In the Central Depression, CPx are present in all the studied sedimentary formations (Table 2). In the Azapa Formation, they are dark or light green, translucent, pseudo-prismatic or angular and without inclusions. In the Latagualla and El Diablo Formations, they are dark green, translucent, prismatic, angular or pseudo-prismatic, occasionally rounded and contain Fe–Ti oxide inclusions. The CPx of these series are always associated with OPx (enstatite), except in samples L1 and A17.

In the Altiplano, CPx are present in most samples but are rarely abundant (Table 1). CPx are translucent, free of inclusions, angular or prismatic (B33, B34, B58) and occasionally subrounded. The colour is strongly dark green, but in some samples rare light green grains are observed (B61, B62, B63).

In Table 2, the representative chemical compositions of the analyzed CPx are shown. CPx from the Central Depression have high SiO_2 (48.98–53.57 wt.%), CaO (18.69–23.35 wt.%) and MgO (13.06–17.89 wt.%) contents, moderate Al_2O_3 (0.58–7.03 wt.%) and total FeO (1.77–14.77 wt.%) contents, and low TiO_2 (0.06–0.97 wt.%), Na_2O (0.19–0.59 wt.%) and MnO (0.04–0.80 wt.%) contents. The CPx of the Azapa Formation have slightly higher X_{Mg} ($Mg/[Mg+Fe^{2+}]$) (0.76–0.97) content than those of the Latagualla and El Diablo (0.68–0.87) Formations. The composition of CPx from the Altiplano basins (Table 2) exhibit a slightly lower SiO_2 (45.90–53.36 wt.%), MgO (12.13–17.82 wt.%), total FeO (1.69–14.00 wt.%) and MnO (0.01–0.64 wt.%) contents, and higher contents of CaO (20.62–23.66 wt.%), Al_2O_3 (0.40–7.29 wt.%), TiO_2 (0.02–2.02 wt.%) and Na_2O (0.16–0.70 wt.%) than those from the Central Depression. CPx from the Central Depression plot mainly in the augite field of the $Ca_2Si_2O_6$–$Mg_2Si_2O_6$–$Fe_2Si_2O_6$ diagram of Morimoto (1988) (Fig. 4a), and rarely in the diopside field (Azapa Formation), whereas those from the Altiplano plot mainly in the diopside field and only rarely in the augite field (Fig. 4a).

The augite–diopsides of the Azapa Formation are associated with andradite, grossular and actinolite indicating a metamorphic origin, probably an amphibolite of basaltic protolith. In the Latagualla and El Diablo Formations, the augite–enstatite–forsterite assemblage and the idiomorphic habit of the grains indicate a basalt–andesite source. Augite and enstatite are common minerals of various volcanic rocks, but the presence of forsterite ($Fo_{80}Fa_{20}$), which crystallizes in equilibrium with augite and occurs as phenocrysts in mafic subalkaline lavas (Deer et al., 1982), points to a mafic volcanic source rock. Enstatite is also a mineral present in mafic rocks and occurs also as phenocrysts in subalkaline basalt–andesites (Nakamura and Kushiro, 1970) where it is commonly associated with olivine, augite and spinel (Deer et al., 1978). Thus, the augite–enstatite–forsterite assemblage found in the Latagualla and El Diablo Formations is a clear signature of basalt–andesite source. Previous experimental work has determined the temperature dependence of the distribution of Fe^{2+} and Mg^{2+} between olivine and OPx (e.g., Nafziger and Muan, 1967; Wood, 1975), which has long been observed in natural rocks (e.g., Bartholomé, 1962). Here, X_{Mg} ($Mg/[Mg+Fe^{2+}]$) for OPx associated with olivine varies between 0.61 and 0.82 and is slightly lower than that of the olivine X_{Mg} (0.69–0.87). Calculations for $T=1000$ °C show that olivine with $X_{Mg}=0.70$–0.87 can be in equilibrium with OPx having $X_{Mg}=0.7$–0.8, but not with OPx in the 0.6–0.7 range observed here (Holland and Powell, 1998). This implies that these less magnesian OPx were not associated with olivine in a common source rock. The samples with these OPx have also accessory hornblende (magnesiohornblende, magnesiohastingsite, pargasite) and phlogopite, which

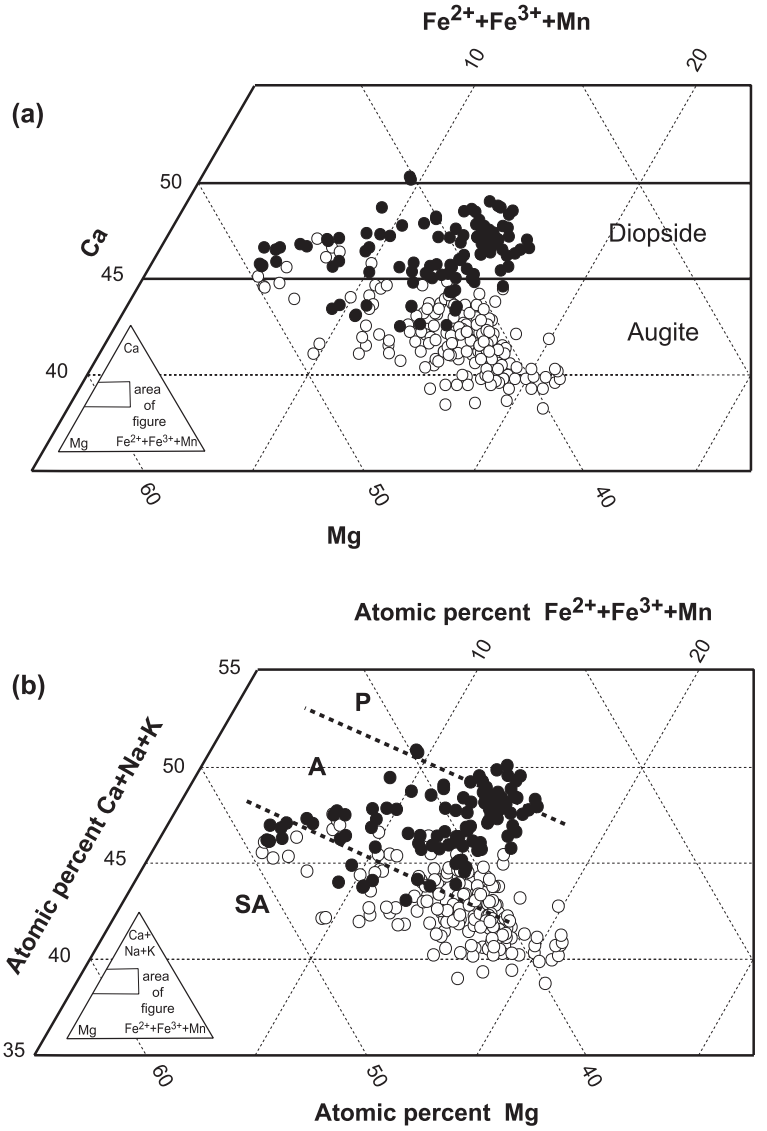

Fig. 4. (a) Classification diagram of clinopyroxenes (Morimoto, 1988) from the Central Depression ($n = 182$; open circles) and Altiplano ($n = 115$; filled circles) sandstones. (b) The same data plotted on a discrimination diagram for clinopyroxenes from subalkaline (SA), alkaline (A) and peralkaline (P) magma suites (after Le Bas, 1962).

defining an intermediate igneous source (dacites-rhyodacites) (Deer et al., 1978). It is probable that OPx with $X_{Mg} = 0.7-0.8$ are associated with them and have the same source.

In the course of crystallization of a mafic volcanic magma, phenocrysts of pyroxenes precipitate earlier and exhibit higher X_{Mg} than the groundmass of the rocks. Consequently, there is no rigorous correlation between the X_{Mg} in whole-rock and in the CPx. However, there is a general trend of decreasing X_{Mg} in the pyroxenes and the whole-rock with progressive differentiation and these values are constrained within a given field for a given stage of differentiation. The field for both Andean andesites and experimental data is outlined in Fig. 5 (data after Kawamoto, 1996; García, 1997, 2001; Legros, 1998). The plot of the

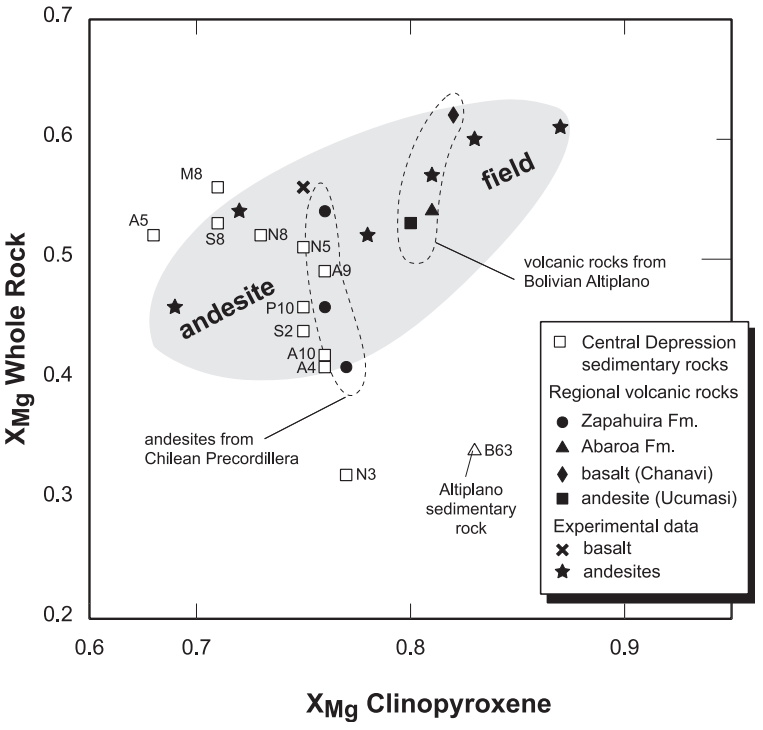

Fig. 5. X_{Mg} ($Mg/[Mg+Fe^{2+}]$) of the whole-rock relative to X_{Mg} of the clinopyroxenes from the studied sandstones and regional and experimental volcanic rocks (after Kawamoto, 1996; Legros, 1998; García, 1997, 2001). Grey field shows the andesite domain.

volcaniclastic sandstones in the X_{Mg} (whole-rock) vs. X_{Mg} (CPx) diagram (Fig. 5) suggests homogeneity only of the source rocks for the Central Depression, the only suitable analysed samples of the Altiplano formations plot apart from this domain. Thus, the Central Depression sandstones with an andesitic mineralogy and whole-rock composition plot within the andesitic field and they most probably derive from a homogeneous andesitic source rock.

The pyroxenes (augites, enstatites) from the youngest sedimentary rocks (Latagualla and El Diablo Formations) have a low Ti content (< 1 wt.%, Table 2), but contain abundant Fe–Ti oxide inclusions. This suggests source rocks originating from an initially Fe–Ti-rich magma in which early crystallization of Fe–Ti oxides was the cause of the Ti-poor composition of the residual magma. This mechanism defines a calc-alkaline trend for the mafic volcanic source of the Latagualla and El Diablo Formations.

Thus, the mineral assemblage, mineral habit and composition of the grains all indicate calc-alkaline volcanic source rock of mafic (basalt–andesite) and intermediate (dacite–rhyodacite) chemical affinity for these formations. These sources were probably the Miocene basalts, andesites and dacites occurring in the Western Cordillera (Seguel, 1991; García, 2001).

The heavy minerals from the Altiplano series (the Berenguela, Mauri, Caquiaviri and Pomata Formations), except the Coniri Formation, show some similarities to those of the Latagualla and El Diablo Formations. The diopside, hornblende, biotite, titanite and apatite (Table 1) exhibit volcanic mineral habits, with slightly rounded idiomorphic grains. Neither olivine nor enstatite is present and the CPx are free from Fe–Ti oxide inclusions. The assemblage of hornblende + phlogopite + titanite + apatite suggests a volcanic source of intermediate (rhyodacite) to felsic (rhyolite) sources whereas the CPx suggest a mafic (basalt–andesite) one.

Leterrier et al. (1982) used the Ca, Na and Ti concentrations in a set of 1225 CPx to discriminate, with a confidence level higher than 80%, between

pyroxenes phenocrysts from alkali basalts (field A), orogenic basalts (calc-alkaline) and non-orogenic tholeiites (field T) (Fig. 6). These diagrams have been applied to paleovolcanic metabasites and can also be applied to old mafic volcaniclastics, when CPx phenocrysts have been well preserved (Nisbet and Pearce, 1977; Krawinkel et al., 1999). Assuming that the CPx studied here originated from mafic sources, their compositions have been plotted in the Ti vs. (Na + Ca) diagram of Leterrier et al. (1982). The CPx from the Central Depression show a subalkaline affinity (Fig. 6). The CPx from the Azapa Formation are nearest to the alkaline field suggesting that the protolith of the amphibolite was a more alkali-rich volcanic rock. The majority of the CPx from the Altiplano plot within the alkali basalt field, most being from the Mauri Basin [Berenguela (sample B32) and Mauri (sample B63) Formations] (Fig. 6). Nevertheless, the CPx from the Coniri (B49, B50) and Caquiaviri (B56, B57) Formations and some grains from the Mauri Formation (B61, B62), in the Corque Basin, plot outside the alkaline confidence field (Fig. 6). These pyroxenes have the (Na + Ca) values characteristic of alkaline pyroxenes, but their Ti content is low for alkaline magmas. Either they did not crystallize from a mafic source or a Ti-bearing phase crystallized before the CPx, the Ti content of the magma was depleted. This early mineral phase was probably titanite, which is abundant in the Altiplano series.

Kushiro (1960) and Le Bas (1962) showed that the Al content of calcic pyroxene (augite and diopside) increases with decreasing SiO_2 concentration in the magma. Le Bas (1962) also demonstrated a distinctive relationship between the Al_2O_3 and SiO_2 contents in CPx from subalkaline, alkaline and peralkaline rock suites (Figs. 4b and 7). In the Al_2O_3 vs. SiO_2 covariation diagram of Le Bas (1962), CPx from the Central Depression plot within the subalkaline field (Fig. 7). Concerning the Altiplano CPx, the samples from the Caquiaviri Formation also plot in the subalkaline field, whereas those from the Berenguela, Mauri and Pomata Formations are spread in the

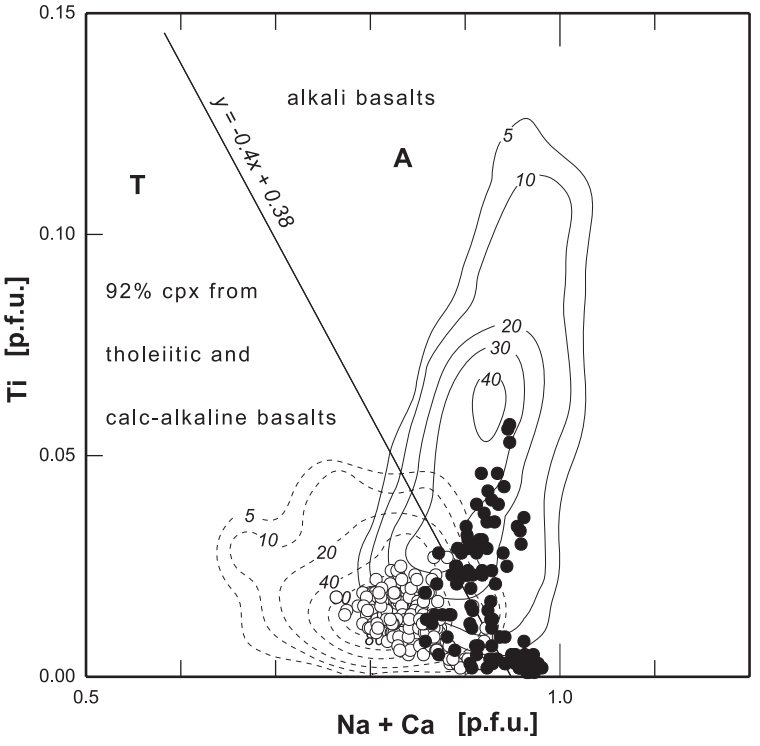

Fig. 6. Discrimination diagram for clinopyroxenes from alkali-basalts (A) and subalkaline basalts (T) (after Leterrier et al., 1982) from the Central Depression ($n = 182$; open circles) and Altiplano ($n = 115$; filled circles) sedimentary rocks.

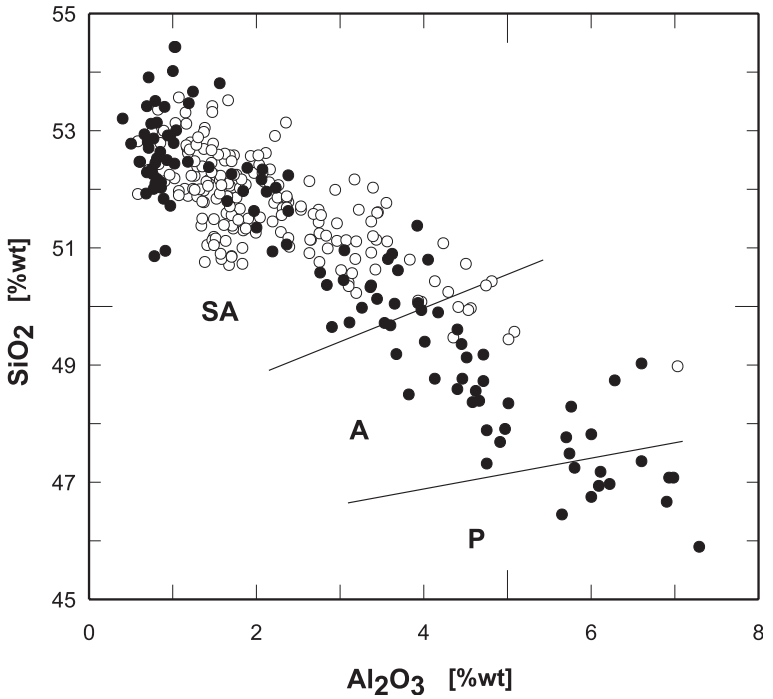

Fig. 7. Discrimination diagram (Al_2O_3) vs. (SiO_2) for clinopyroxenes from subalkaline (SA), alkaline (A) and peralkaline (PA) magma suites (after Le Bas, 1962). Data from the Central Depression ($n = 182$; open circles) and Altiplano ($n = 115$; filled circles) sandstones.

subalkaline, alkaline and peralkaline fields (Fig. 7). Compared to the other CPx, those from the Berenguela and Mauri Formations (B32, B63) exhibit a higher Al_2O_3 content characteristic of minerals from alkaline to peralkaline magmas. These results suggest the occurrence of volcanic sources at various stages of the magmatic evolution. Mineral compositions plotting outside the alkaline field in the Leterrier et al. (1982) diagram (Fig. 6) plot in the subalkaline field of the Le Bas (1962) diagram (Fig. 7), and those plotting within the confidence limits have alkaline affinity in both diagrams. Therefore, CPx from the Corque Basin (Caquiaviri and Mauri 6 Formations) would have crystallized from a subalkaline magma, and the others from an alkaline one.

5.2. Major elements

Major element data (Table 3) show low SiO_2/Al_2O_3 (IM) and high Na_2O/K_2O ratios that indicate greywacke compositions (Pettijohn et al., 1972) for both the Central Depression and the Altiplano samples, except the Coniri (B49, B50) and Caquiaviri (B56, B57) Formations. SiO_2/Al_2O_3 is an approximate indicator of the quartz/feldspar ratio (Moine, 1974) and the low values observed reflect low maturity of the greywackes, mainly for those from the Central Depression (Table 3). In the (Al/3 − K) vs. (Al/3 − Na) diagram, most of the samples plot in the igneous field (Fig. 8; De La Roche, 1968; Moine, 1974), which is coherent with the heavy mineral assemblages. Alteration of igneous rocks can be evaluated in terms of the Chemical Index of Alteration ($CIA = Al_2O_3/[Al_2O_3 + CaO + Na_2O + K_2O]$; Nesbitt and Young, 1982). The average value of 60 obtained for both the greywackes studied and the igneous rocks in this region (data after Geobol, 1995; García, 1997, 2001; Legros, 1998) suggest little weathering. Consequently, it is interesting to verify and quantify the igneous component and to determine the overall nature of the igneous source rocks. The diagrams proposed for the chemical classification of diverse plutonic and volcanic rocks (De La Roche, 1967; Pearce and Cann, 1973; Floyd and Winchester,

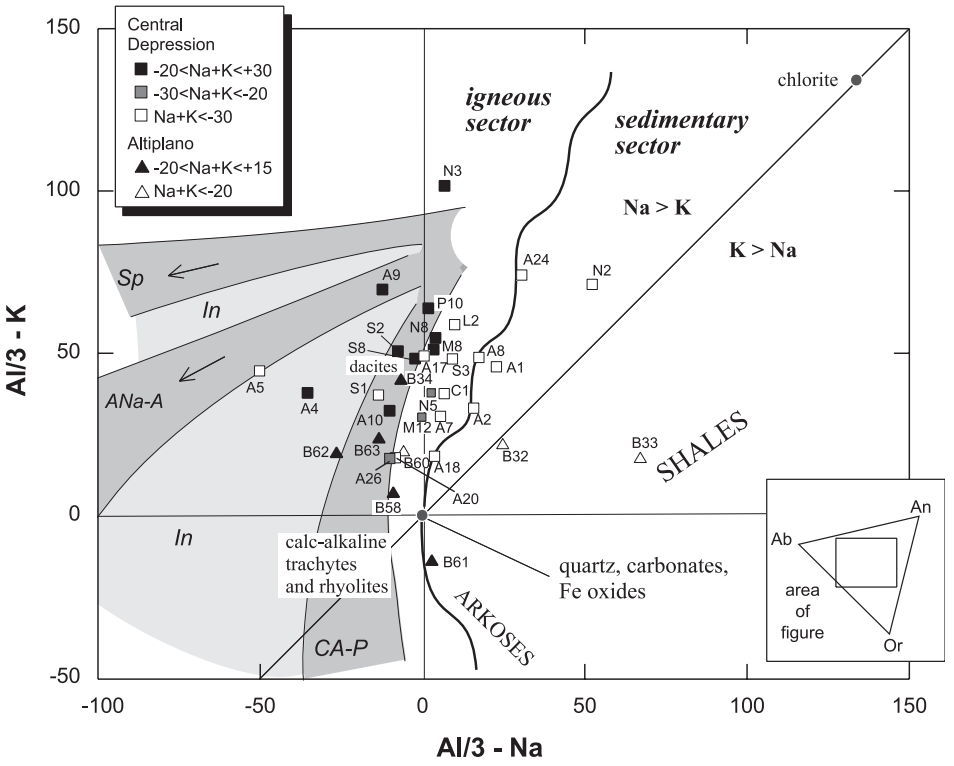

Fig. 8. Discrimination diagram (Al/3 − Na) vs. (Al/3 − K), values in milli-cations (after De La Roche, 1968) for sedimentary rocks from the Central Depression and Altiplano formations. Volcanism: Spilitic (Sp), Na-alkaline Atlantic (Ana-A), calc-alkaline Pacific (CA-P) and intermediate between them (In), Ab: albite, An: anorthite, Or: orthoclase.

1975; Winchester and Floyd, 1977) are well suited to this purpose.

Locally, the cement of the sandstones of the El Diablo Formation in the Camarones Valley contains some smectite and silica (García, 2001) in the fine-grained sedimentary rocks of distal fans. However, the sedimentary deposits studied here are not cemented and their matrix is practically unaltered. Most of them display scarce silty-clay matrix (< 1%), consisting of volcanic glass, samples of which from some representative sandstones of the formations were analyzed by XRD. In most samples, fine material is very scarce and only silt was obtained, the clay matrix being absent. Two main compositional types are apparent: in one group, the diffraction spectrum shows only the presence of essential mineral constituents of the sandstone, i.e., feldspars, quartz, amphibole and pyroxene; in the other group, in addition to these minerals, the diffraction spectrum shows the possible presence of illite or interstratified clay minerals. However, the low intensity of the spectrum indicates a low proportion of these minerals in the matrix and, therefore, in the total sandstone. Only locally, in sandstones with a matrix richer in volcanic ash, does the XRD spectrum indicate the presence of a true clay (nontronite). These last sandstones are those with the lowest alkali contents. Thus, the fact that the rocks with a silty-clay matrix are very scarce, that the

Fig. 9. Whole-rock sedimentary rock compositions compared with those of igneous rocks: (a) [K − (Na + Ca)] vs. [Si/3 − (Na + K + 2/3Ca)], values in milli-cations (after De La Roche, 1967). The segmented lines are curves of the normal alkali surface of igneous rocks. (b) [K − (Na + Ca)] vs. (Na + K). The thick line approximately represents a profile of this surface from N3 to N2 on (a), and the segmented lines and numbers indicate the difference relative to it. Compositions from calc-alkaline igneous rocks in northwestern Bolivia (×) and calc-alkaline igneous rocks in northern Chile (+), all from the western Cordillera, are represented.

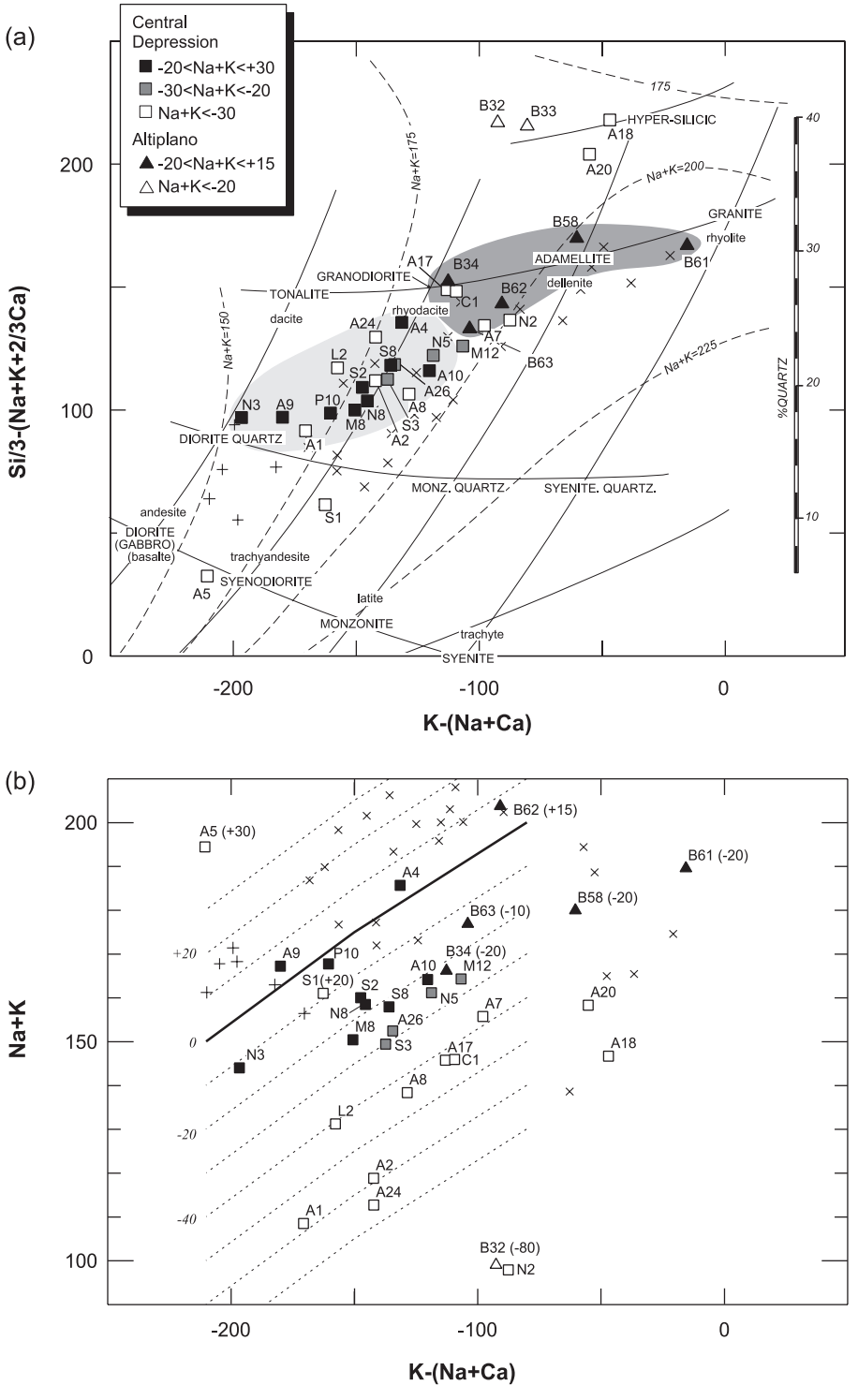
(a)
Central Depression
-20<Na+K<+30
-30<Na+K<-20
Na+K<-30
Altiplano
-20<Na+K<+15
Na+K<-20
Si/3-(Na+K+2/3Ca)
K-(Na+Ca)
200
100
0
-200
-100
0
175
Na+K=175
Na+K=200
Na+K=225
Na+K=150
40
30
20
10
%QUARTZ
HYPER-SILICIC
GRANITE
rhyolite
ADAMELLITE
dellenite
GRANODIORITE
TONALITE
dacite
rhyodacite
DIORITE QUARTZ
MONZ. QUARTZ.
SYENITE. QUARTZ.
andesite
DIORITE (GABBRO) (basalte)
trachyandesite
SYENODIORITE
latite
MONZONITE
trachyte
SYENITE
B32
B33
A18
A20
B58
B61
A17
B34
B62
C1
A24
A4
A7
N2
N5
M12
B63
L2
S8
S2
A10
A26
N3
A9
P10
N8
M8
A8
S3
A2
A1
S1
A5
B32 (-80)
N2
(b)
Na+K
K-(Na+Ca)
200
150
100
-200
-100
0
A5 (+30)
B62 (+15)
B61 (-20)
A4
B58 (-20)
B63 (-10)
+20
0
-20
-40
A9
P10
B34 (-20)
A10
M12
S1(+20)
S2
S8
N5
A7
A20
N8
A26
M8
S3
A17
C1
A18
N3
A8
L2
A2
A24
A1

fraction of matrix altered to smectite is negligible, and that the minerals of igneous origin remain unaltered are evidence that these sedimentary rocks have experienced practically no alteration. Thus, the scarce matrix present cannot have affected the determination of their igneous source rocks.

The samples of igneous affinity with a relatively low (<40%) normative quartz content are plotted in the diagrams for igneous rock classification of De La Roche (1964, 1967) (Fig. 9a). The sandstones of the Central Depression plot mainly as quartz–andesites and rhyodacites, with normative quartz between 15% and 25%, and with Na + K below the surface of normal alkalinity. This is determined by comparing the (Na + K) values of the samples with those of the corresponding plutonic rocks (line labelled "0", Fig. 9b). Two samples (S1 from the Latagualla Formation, and A5 from the El Diablo Formation) plot apart from the trend towards the syenodiorites (trachyandesites) field with normative quartz between 5% and 12% and they are above the normal alkalinity for igneous rocks (Fig. 9a and b). The high ignition loss (IL) and Ca values in these samples relative to the corresponding igneous rocks indicate the presence of calcite in the matrix, and explain their location away from the general trend. In the same diagram, the Altiplano sandstones range between the rhyodacite and rhyolite fields with normative quartz between 25% and 35%, and plot in the alkali-poor region (except for sample B62, which is located above the surface of normal alkalinity, Fig. 9a and b). The alkali index $AI=[(Na_2O+K_2O)/((SiO_2-43)*0.17)]$ proposed for subalkaline rocks (Middlemost, 1975) suggests a greater alkalinity for the volcaniclastic sandstones of the Central Depression (1.99–2.26) compared to those of the Altiplano (1.60–1.86) (Table 3). The alkalinity of the potential source rocks is higher than these values, their AI varying between 2.10 and 2.27 in the calc-alkaline suites from the western side of the Western Cordillera (data after García, 2001) and between 1.62 and 2.74 in calc-alkaline suites from its eastern side (data after Geobol, 1995) (Table 4). Mechanical mineral sorting during transport and undetected, supergene alteration have probably affected the sediments of igneous affinity.

Some samples contain minerals indicating that they come from particular outcrops, which explains their distance from the general tendency as show by the white boxes in Fig. 9b. Sample N2, rich in volcanic ash, contains the clay mineral nontronite that derives from the alteration of volcanic glass, probably from rhyodacitic ignimbrites, according to its position in the diagram of Fig. 9b. The dacitic source deduced from the heavy mineral assemblage has, therefore, been diluted. The samples of the Azapa Formation have metabasites and dacites as a source, thus their overall geochemistry corresponds to a mixture of different rocks. The samples of the Berenguela, Coniri and Caquiaviri Formations also indicate granites and metamorphic source rocks; thus, the andesitic volcanic source gets diluted and is not apparent in the overall geochemistry. This explains why only the geochemistry of the youngest formations of the Central Depression, i.e., Latagualla and El Diablo Formations, and of the Altiplano, i.e., Mauri and Pomata Formations, which derive exclusively from volcanic rocks, is able to evidence this volcanic characteristic.

The CPx were found in samples where the major element composition indicated a felsic affinity; specifically in the youngest sedimentary rocks of the Pomata and Mauri Formations. It is probable that

Table 4
Compositions of calc-alkaline volcanic rocks from western Cordillera and Precordillera

Sample	Western Cordillera (western Bolivia)			Precordillerac (northern Chile)		
	W-418	NJ-36	SK-513	MAL-124	MAL-194	MAL-192
SiO_2	60.30	73.80	64.90	58.34	56.94	58.82
TiO_2	0.85	0.21	0.37	0.67	0.76	0.77
Al_2O_3	16.40	13.80	16.40	18.24	17.47	16.33
Fe_2O_3	5.94	1.23	3.52	6.56	6.84	7.11
MnO	0.09	0.06	0.10	0.06	0.10	0.14
MgO	2.22	0.27	0.39	2.82	3.05	3.47
CaO	4.94	0.87	2.16	6.39	7.44	6.43
Na_2O	4.13	3.93	4.02	4.00	3.61	3.28
K_2O	3.05	4.55	4.42	1.82	2.43	2.38
P_2O_5	0.37	0.05	0.22	0.23	0.22	0.18
IL[a]	1.47	1.16	1.45	0.60	1.40	1.30
AI[b]	2.44	1.62	2.27	2.23	2.55	2.10
X_{Mg}[c]	0.43	0.30	0.18	0.46	0.47	0.49
CIA[d]	0.58	0.60	0.61	0.60	0.56	0.57

Data after Geobol (1995) and García (2001).

[a] IL: Ignition Loss.

[b] AI (alkalinity index)=$(Na_2O+K_2O)/((SiO_2-43)*0.17)$ (after Middlemost, 1975).

[c] $X_{Mg}=Mg/(Mg+Fe)$.

[d] $CIA=Al_2O_3/(Al_2O_3+CaO+Na_2O+K_2O)$ (after Nesbitt and Young, 1982).

these samples correspond to a mixture of a main felsic source with a minor contribution from a mafic source. The alkaline mafic source, evidenced by the CPx, is probably diluted by the more abundant felsic source. The latter would have contributed the CPx to the Mauri and Corque Basins.

Following this approach, we have verified the igneous affinity and the overall geochemistry of the source rocks of the youngest formations from the Central Depression and the Altiplano. Nine samples with Na + K ~ ± 20 relative to the surface of normal alkalinity (Fig. 9b) from the Central Depression (Latagualla and El Diablo Formations) and five from the Altiplano (Mauri and Pomata Formations) are derived from igneous source rocks (Fig. 10), based on their compositions close to the volcanic rocks of the Western Cordillera (Fig. 9a). However, some hypo-alkaline samples and the sandstones with normative quartz higher than 40% (Fig. 9) also exhibit heavy minerals of igneous origin (Table 1). They probably reflect the mixing of rocks and their geochemistry does not represent the overall composition of a particular volcanic source rock. Thus, both the geochemical and the mineralogical features must be taken into account in order to infer the characteristics of the source rocks.

5.3. Trace elements

Unlike those from the Altiplano, the sandstones from the Central Depression show rather homogenous trace element concentrations (Table 3). Nevertheless, the La/Yb in the El Diablo and the Latagualla Formations (mean La/Yb = 15.49) is distinctly higher than that in the Azapa Formation (mean La/Yb = 11.62), indicating a more differentiated magmatic source rock (Wilson, 1989). This difference is even greater in the sandstones of the Mauri Formation (mean La/Yb = 35.78) (Table 3). This increase in the La/Yb reflects an increase in the light rare earth element/heavy rare earth element (LREE/HREE) ratio and indicates a more differentiated magmatic source rock for the Azapa Formation, and even more so for the Mauri Formation. Another interesting observation is the higher concentrations of Ta and Nb in the Altiplano sandstones (Ta = 0.37–13.52, Nb = 4.85–47.97) compared to those in the Central Depression (Ta = 0.48–2.21, Nb = 6.67–11.73), pointing to a

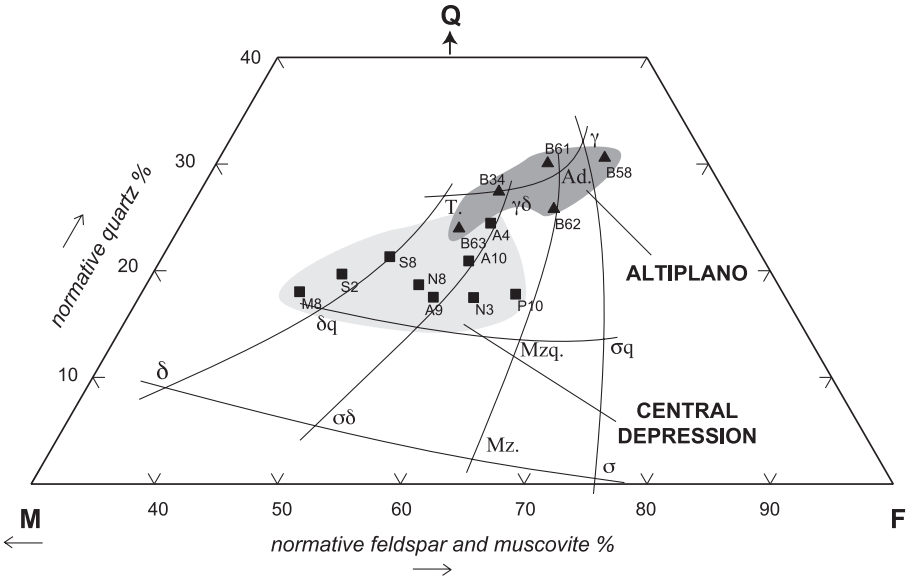

Fig. 10. Whole-rock sedimentary rock compositions from the Central Depression (filled boxes) and the Altiplano (filled triangles) plotted on a triangular diagram of normative quartz (Q), feldspar-muscovite (F) and ferromagnesian (M) minerals (after Moine, 1974); with Q=[Si/3 – (Na + K + 2/3Ca)/5.55], M=[Fe + Mg + Ti/5.55] and F=[100 – (Q + M)] in milli-cations. Symbols used as in Fig. 9. δ: diorite, σδ: syeno-diorite, Mz.: Monzonite, σ: syenite, δq: quartz-diorite, Mzq.: quartz-monzonite, σq: quartz-syenite, T.: Tonalite, γδ: granodiorite, Ad.: adamellite, γ: granite.

higher degree of magmatic differentiation of the Altiplano source rocks than those from the Central Depression (Pearce et al., 1984; Thiéblemont, 1999).

Winchester and Floyd (1977) developed immobile element diagrams to determine the differentiation stage and alkalinity of volcanic rocks. Their [Nb/Y] (differentiation index) vs. (Zr/TiO_2) (alkalinity index) diagram (Pearce and Cann, 1973; Floyd and Winchester, 1975) is especially interesting because it is independent of the SiO_2 and alkali contents of the rocks. When this diagram is used, two igneous suites are apparent: a subalkaline basalt–andesite–dacite suite for the Central Depression and an alkaline basalt–trachyte suite for the Altiplano (Fig. 11). It is interesting to note that the alkali-poor samples from the Central Depression (Fig. 9b) plot in this diagram in the subalkaline domain very close to the overall tendency of the more alkali-rich samples from this region. The same contrast between the two regions was observed in the discrimination diagrams of clinopyroxenes (Le Bas, 1962; Leterrier et al., 1982) (Figs. 4b, 6 and 7). This discrimination is diffuse on the major element diagram for igneous classification (De La Roche, 1967, 1968) (Figs. 8 and 9a), probably due to alkali (Na, K) mobility and mixing of source rocks.

5.4. Discussion: mineralogical and geochemical relations

Although the study of the composition of sediment is a complex subject, the identification of the rock sources of sedimentary deposits based on mineralogical and geochemical analyses constitutes a reasonable approach. In this study, the heavy mineral assemblages indicate an intermediate volcanic source for the oldest sedimentary deposits of the Central Depression and an intermediate to mafic volcanic source for the youngest sedimentary rocks of this basin. The heavy mineral assemblages in sandstones of the Altiplano show intermediate and felsic igneous sources, locally mafic. The chemistry of the CPx indicates a subalkaline character for the mafic source of the Central Depression and a mainly alkaline one for those of the Mauri Basin of the Altiplano and, locally, a minor subalkaline component for those of

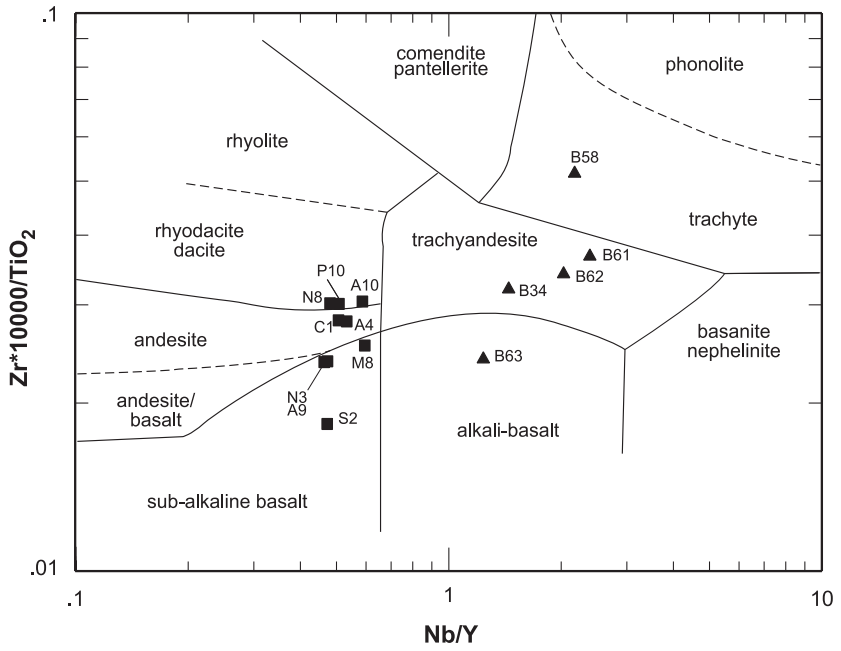

Fig. 11. Whole-rock sedimentary rock compositions from Central Depression (filled boxes) and Altiplano (filled triangles) plotted on the discrimination diagram [Zr∗10,000/(%TiO_2)] vs. [Nb/Y] of volcanic rocks, values in ppm (after Winchester and Floyd, 1977). Symbols used as in Fig. 9.

the Corque Basin. The trace elements Nb, Y, Zr and Ti mark the same global difference between these two groups, subalkaline and alkaline respectively, whereas Ta, Nb, La and Yb indicate a greater crustal contamination in the alkaline group. The major elements, from whole-rock analyses, reveal the same tendencies as shown by the heavy mineral assemblages for these two groups. Only a few samples plot away from the general trend, with a more mafic character in the first group and a more felsic one in the second, probably due to the mechanical concentration of minerals during transport. The overall compositions shown by the major elements do not demonstrate the difference in alkalinity shown by the CPx and the trace elements. This is probably because of the mixture of source rocks that dilutes its particular characteristic and also to the mobility of the alkaline elements (Na, K) during the sedimentary processes. Therefore, we can deduce that the volcanic source zone of the sedimentary rocks from the Altiplano was rhyolitic to rhyodacitic, locally mafic alkaline character in the Mauri Basin and locally of subalkaline in the Corque Basin. In the Central Depression, this source was composed of rhyodacitic to basaltic–andesitic rocks of a calc-alkaline character, less contaminated by the continental crust relative to the source rocks of the Altiplano.

6. Synthesis and regional correlation. Erosion on the Western or Eastern Cordillera?

In summary, we have determined that the source rocks of the continental Neogene sedimentary rocks of the Central Depression, and those of the Corque Basin in the central region of the Altiplano are calc-alkaline, mafic to intermediate volcanic rocks, whereas the source rocks for the similarly continental Neogene sedimentary rocks of the Mauri Basin, on the western edge of the Altiplano, are alkaline intermediate to felsic volcanic rocks. The volcanic source(s) of the sedimentary rocks of the Central Depression broadly correspond(s) to the Oligocene–Miocene andesitic–dacitic lavas and rhyolitic ignimbrites of medium-K calc-alkaline and locally shoshonitic character, located in the western Cordillera (Thorpe and Francis, 1979; Harmon et al., 1984; Sébrier and Soler, 1991; García, 2001).

Alkaline and shoshonitic lavas have also been documented in the Mauri Basin, from the lower Upper Oligocene–Lower Miocene members (1–4) of the Mauri and Abaroa Formations (Lavenu et al., 1989; Geobol, 1995), which are confined to the eastern edge of the Western Cordillera. Similar rocks are also present in the equivalent Tambillo and Rondal Formations (Fornari et al., 1993, 1996) on the western edge of the Eastern Cordillera. The Eastern Cordillera is geographically too far away to constitute the source of the alkaline volcaniclastic sedimentary rocks in the Mauri Basin. Considering their geographic location, it is more probable, that the Berenguela and Mauri Formations originated from alkaline volcanic deposits formed in the Western Cordillera during the development of the Mauri Basin.

These results indicate that for the Late Oligocene–Early Miocene, magmatism of different characteristics existed on one side to the other of the Western Cordillera, calc-alkaline at the western margin contributing with sediments towards the Central Depression and alkaline at the eastern margin contributing towards the Mauri Basin. This situation probably reflects a thinner continental crust under the western border than under in the eastern border of the Western Cordillera, a fact that might have influenced the geochemistry of the ascending magmas. Alkaline lavas are documented on the landward side of the volcanic belt in the Andean Cordillera (Thorpe et al., 1982) and they are related to an extensional tectonic regimes similar to that of back-arc basins (Wilson, 1989).

The source rocks for the Lower Miocene–Pliocene sedimentary rocks (~ 14–5 Ma) of the Corque Basin can come from either the Western or Eastern Cordillera. In the Western Cordillera, Lower Miocene–Pliocene volcanic deposits of calc-alkaline character (Soler and Jiménez, 1993) have been described in members 5–6 of the Mauri Formation, the Serhke Formation and the Pérez Ignimbrite (Lavenu et al., 1989; Geobol, 1995). In the Eastern Cordillera, Miocene felsic high-K calc-alkaline volcanic rocks also exist in southern Bolivia, i.e., Cerro Morokho, Cerro Bonete and Lípez (Fornari et al., 1993) far from the studied area (Fig. 1). Two arguments support a derivation from the Eastern Cordillera:

(1) Extensive felsic calc-alkaline, high-K lava and ignimbrite provinces, lie along the western edges of

the Eastern Cordillera from southern Peru (Macusani; Pichavant et al., 1988a,b) into Bolivia (Morococala and Los Frailes; Schneider and Halls, 1985; Ericksen et al., 1990; Luedke et al., 1990; Leroy and Jiménez, 1996; Morgan et al., 1998) (Fig. 1). However, in an extensive sector around La Paz, immediately east of the study region, these felsic volcanics are not preserved (e.g., Morgan et al., 1998; Grant et al., 1979) and only a few shoshonitic lavas are exposed (Redwood and Rice, 1997; Legros, 1998). It is possible that the felsic volcanics have been eroded leaving only the plutons of the magmatic system (Illimani and Quimsa Cruz). Therefore, the sedimentary deposits accumulated in the Corque Basin would be the evidence for their former existence and later erosion.

(2) The volcaniclastic sedimentary rocks of the Early Miocene in the Mauri Basin, located between the Western Cordillera and the Corque Basin, indicate that the source rocks were alkaline. The sedimentary rocks of the same age in the Corque Basin indicate that the source rocks were calc-alkaline. Consequently, this sedimentary material in the Corque Basin could not have come from the west.

7. Conclusion

We have shown that bulk geochemical analyses of sedimentary rocks together with accurate analyses of heavy mineral grains can help in the reconstruction of paleo-relief. The data suggest that, during the Late Oligocene–Early Miocene, alkaline magmatism at the eastern slope of the Western Cordillera contributed sedimentary material only to the Mauri Basin, whereas calc-alkaline magmatism at the western slope of the Western Cordillera contributed sedimentary material to the Central Depression during the Late Oligocene–Late Miocene. The results also suggest that the complete erosion of a Miocene–Pliocene felsic calc-alkaline volcanic pile along the western edge of the Eastern Cordillera provided the sedimentary material that accumulated in the Corque Basin.

Acknowledgements

The authors are grateful to Philippe de Parseval, Michel Valladon and Remi Freydier of the LMTG (Toulouse) and Eugenia Fonseca of the SERNAGEOMIN (Santiago) for valuable help in assembling the data file; to Didier Beziat, Luis Aguirre and Jacobus Le Roux for fruitful discussions; and the Universidad de Chile and IRD for financial support of this work. This manuscript greatly benefited from useful comments by Andrew C. Morton and Peter A. Cawood.

References

Ahlfeld, F., 1946. Geología de Bolivia. Rev. Mus. La Planta 3 (19), 5.370.

Alpers, C., Brimhall, G., 1988. Middle miocene climatic change in the atacama desert, northern Chile: evidence from supergene mineralization at La Escondida. Bull. Geol. Soc. Am. 100, 1640–1656.

Argast, S., Donnelly, T., 1987. The chemical discrimination of clastic sedimentary components. J. Sediment. Petrol. 57, 813–823.

Ascarrunz, R., Claure, L., Revollo, R., 1967. Hoja geológica N° 5942, "Corocoro". Publ. Serv. Geol. Boliv. (GEOBOL).

Bartholomé, P., 1962. Iron–magnesium ratio in associated pyroxenes and olivines. Bull. Geol. Soc. Am., Buddington, 1–20.

Bhatia, M., 1983. Plate tectonics and geochemical composition of sandstones. J. Geol. 91, 611–627.

Bhatia, M., Crook, K., 1986. Trace element characteristics of graywackes and tectonic setting discrimination of sedimentary basins. Contrib. Mineral. Petrol. 92, 181–193.

Cameron, M., Papike, J., 1981. Structural and chemical variations in pyroxenes. Am. Mineral. 66, 1–50.

Cawood, P., 1983. Modal composition and detrital clinopyroxene geochemistry of lithic sandstones from the New England Fold Belt (east Australia): a Paleozoic forearc terrane. Geol. Soc. Amer. Bull. 94, 1199–1214.

Cawood, P.A., 1991a. Nature and record of igneous activity in the Tonga arc, SW Pacific, deduced from the phase chemistry of derived detrital grains. In: Morton, A.C., Todd, S.P., Haughton, P.D.W. (Eds.), Developments in Sedimentary Provenance Studies. Spec. Publ.-Geol. Soc. Lond., vol. 57, pp. 305–321.

Cawood, P.A., 1991b. Characterization of intra-oceanic magmatic arc source terranes by provenance studies of derived sediments. N.Z. J. Geol. Geophys. 34, 347–358.

De La Roche, H., 1964. Sur l'expression graphique des relations entre la composition chimique et la composition minéralogique quantitative des roches cristallines. Présentation d'un diagramme destiné à l'étude chimico-minéralogique des massifs granitiques ou granodioritiques. Application aux Vosges cristallines. Sci. Terre Fr. 9, 293–337.

De La Roche, H., 1967. Caractères chimiques généraux et classification des roches charnockitiques plutoniques. Sci. Terre Fr., T. XII (3), 207–223.

De La Roche, H., 1968. Comportement géchimique différentiel de Na, K et Al dans les formations volcaniques et sédimentaires. Un guide por l'étude des formations métamorphiques et plutoniques. C.R. Acad. Sci. Fr. 267 (D), 39–42.

Deer, W.A., Howie, R.A., Zussmann, J., 1978. Rock-forming minerals, volume 2A. Single-Chain Silicates, 2nd ed. Wiley, New York.

Deer, W.A., Howie, R.A., Zussmann, J., 1982. Rock-forming minerals, volume 1A. Orthosilicates, 2nd ed. Wiley, New York.

Ericksen, G.E., Luedke, R.G., Smith, R.L., Koeppen, R.P., Urquidi, F., 1990. Peraluminous igneous rocks of the Bolivian tin belt. Episodes 13, 3–7.

Farías, M., Charrier, R., Comte, D., Martinod, J., Pinto, L., Hérail, G., 2002. Active Late Cenozoic flexures in the Precordillera in northern Chile: correlation with shallow seismic activity, and implications for the uplift of the Altiplano. EOS. Trans. American Geophysical Union 83 (47) Fall Meeting Suppl., Abstract T51A-1136.

Floyd, P., Winchester, J., 1975. Magma type and tectonic setting discrimination using immobile elements. Earth Planet. Sci. Lett. 27, 211–218.

Fornari, M., Pozzo, L., Soler, P., Bailly, L., Leroy, J., Bonhomme, M., 1993. Miocene volcanic centers in the southern Altiplano of Bolivia. The Cerro Morokho and Cerro Bonete area (Sur Lipez). Proceedings 2nd International Symposium on Andean Geodynamics, Oxford (UK), pp. 363–366.

Fornari, M., Espinoza, F., Baldellon, E., Soler, P., 1996. Late Oligocene–Early Miocene alkaline magmatism in the central Altiplano of Bolivia. Proceedings 3rd International Symposium on Andean Geodynamics, Saint-Malo (Fr.), pp. 567–570.

García, M., 1997. Le volcanisme calco-alcalin oligo-miocène des Andes Centrales (Nord du Chili): implications sur l'orogénèse andine. Mémoire de D.E.A., Univ. Grenoble 1 (France), 30 pp.

García, M., 2001. Evolution oligo–néogène de l'Altiplano Occidental (arc et avant-arc des Andes d'Arica, 18°–19°S). Tectonique, volcanisme, sédimentation, géomorphologie et bilan érosion–sédimentation. PhD thesis, Univ Joseph Fourier, Grenoble 1 (Fr.), 178 pp.

García, M., Hérail, G., Charrier, R., 1999. Age and structure of the Oxaya anticline: a major feature of the Miocene compressive structures of northernmost Chile. Proceedings 4th International Symposium on Andean Geodynamics, IRD editions, Goettingen (Germany), pp. 249–252.

Geobol, 1995. Evolución petrológica del volcanismo neógeno Berenguela-Charaña. Boletin Geológico No. 6, 93 pp.

Grant, J.N., Halls, C., Avila-Salinas, W., Snelling, N.J., 1979. K–Ar ages of igneous rocks and mineralization in part of the Bolivian Tin Belt. Econ. Geol. 74, 838–851.

Harmon, R.S., Barreiro, B.A., Moorbath, S., Hoefs, J., Francis, P.W., Thorpe, R.S., Deruelle, B., McHugh, J., Viglino, J.A., 1984. Regional O-, Sr-, and Pb-isotope relationships in Late Cenozoic calc-alkaline lavas of the Andean Cordillera. J. Geol. Soc. (Lond.) 141, 803–822.

Hérail, G., Rochat, Ph., Baby, P., Aranibar, O., Lavenu, A., Mascle, G., 1997. El Altiplano norte de Bolivia: Evolución geológica terciaria. In: Charrier, R. (Ed.), El Altiplano. Ciencia y Conciencia en los Andes. Univ. Chile, Santiago, pp. 33–44.

Hérail, G., Charrier, R., García, M., Rochat, Ph., Riquelme R. (in preparation). Late Cenozoic tectonic and geomorphologic evolution in the Northern Chilean high Andes.

Holland, T.J.B., Powell, R., 1998. An internally consistent thermodynamic data set for phases of petrological interest. J. Metamorph. Geol. 16, 309–343.

Isacks, B., 1988. Uplift of the central Andean plateau and bending of the Bolivian orocline. J. Geophys. Res. 94 (B4), 3891–3905.

Kawamoto, T., 1996. Experimental constraints on differentiation and H_2O abundance of calc-alkaline magmas. Earth Planet. Sci. Lett. 144, 577–589.

Krawinkel, H., Wozazek, S., Krawinkel, J., Hellmann, W., 1999. Heavy-mineral analysis and clinopyroxene geochemistry applied to provenance analysis of lithic sandstones from the Azuero-Soná Complex (NW Panama). Sediment. Geol. 124, 149–168.

Kushiro, I., 1960. Si–Al relations in clinopyroxenes from igneous rocks. Am. J. Sci. 258, 548–554.

Lamb, S., Hoke, L., Kennan, L., Dewey, J., 1997. Cenozoic evolution of the Central Andes in Bolivia and northern Chile. In: Burg, J., Ford, M. (Eds.), Orogeny Through Time. Spec. Publ.-Geol. Soc. Lond., vol. 121, pp. 237–264.

Lavenu, A., Bonhomme, M., Vatin-Peignon, N., Pachtère, P., 1989. Neogene magmatism in the Bolivian Andes between 16° and 18°S. Stratigraphy and K–Ar geochronology. J. South Am. Earth Sci. 2, 35–47.

Le Bas, M., 1962. The role of aluminium in igneous clinopyroxenes with relation to their parentage. Am. J. Sci. 260, 267–288.

Legros, P., 1998. Le magmatisme néogène d'arrière-arc de l'Altiplano bolivien: Pétrologie, géochimie et relation avec la structure litospherique des Andes Centrales. PhD thesis, Université de droit, d'économie et des sciences d'Aix-Marseille (Fr.), 167 pp.

Leroy, J.L., Jiménez, N., 1996. Le volcanisme de la bordure occidental de la Meseta de Los Frailes (Bolivie); un jabon représentatif du volcanisme andin depuis l'Oligocene supérieur. Bull. Soc. Géol. Fr. 167, 211–226.

Leterrier, J., Maury, R., Thonon, P., Girard, D., Marchal, M., 1982. Clinopyroxene composition as a method of identification of the magmatic affinities of paleo-volcanic series. Earth Planet. Sci. Lett. 59, 139–154.

Luedke, R., Koeppen, R., Flores A., Espinosa, O., 1990. Reconnaissance geologic map of the Morococala volcanic field, Bolivia. U.S. Geological Survey Miscellaneous Investigations Map I-2014, scale 1:100.000.

Mange, M.A., Maurer, H.F.W., 1991. Schwerminerale in Farbe Enke, Verlag, Stuttgart. 148 pp.

Marshall, L., Swisher, C., Lavenu, A., Hoffstetter, R., Curtis, G., 1992. Geochronology of the mammal-bearing Late Cenozoic on the northern Altiplano, Bolivia. J. South Am. Earth Sci. 5, 1–19.

Masek, J., Isacks, B., Gubbels, T., Fielding, E., 1994. Erosion and tectonics at the margins of continental plateaus. J. Geophys. Res. 99 (B7), 13941–13956.

Middlemost, E.A.K., 1975. The basalt clan. Earth-Sci. Rev. 11, 337–364.

Moine, B., 1974. Caractères de sédimentation et de métamorphisme des séries précambriennes épizonales à catazonales du centre de Madagascar (Région d'Ambatofinandrahana). Mémoire, vol. 31. Université de Nancy, France 293 pp.

Montes de Oca, I., Sirvas, F., Torres, E., 1963. Hoja geológica N° 5742 "Santiago de Machaca". Publ. Serv. Geol. Boliv.

Morgan, G., London, D., Luedke, R., 1998. Petrochemistry of Late Miocene peraluminous silicic volcanic rocks from Morococala field, Bolivia. J. Petrol. 39, 601–632.

Morimoto, N., 1988. Nomenclature of pyroxenes. Mineral. Mag. 52, 535–550.

Morris, P., 1988. Volcanic arc reconstruction using discriminant function analysis of detrital clinopyroxene and amphibole from the New England Fold Belt, Eastern Australia. J. Geol. 96, 299–311.

Morton, A.C., 1991. Geochemical studies of detrital heavy minerals and their application to provenance research. In: Morton, A.C., Todd, S.P., Haughton, P.D.W. (Eds.), Developments in Sedimentary Provenance Studies. Spec. Publ.-Geol. Soc. Lond., vol. 57, pp. 31–45.

Muñoz, N., Charrier, R., 1996. Uplift of the western border of the Altiplano on a west-vergent thrust system, northern Chile. J. South Am. Earth Sci. 9 (3/4), 171–181.

Nafziger, R.H., Muan, A., 1967. Equilibrium phase compositions and thermodynamic properties of olivines and pyroxenes in the system MgO–'FeO'–SiO_2. Am. Mineral. 52, 1364–1385.

Naranjo, J., Paskoff, I., 1985. Evolución cenozoica del piedemonte andino en la Pampa del Tamarugal, norte de Chile (18°–21°S). In: Proceedings 4th Congreso Geológico Chileno, Depto. Geociencias (Universidad del Norte), Antofagasta, vol. 4, pp. 149–165.

Nakamura, Y., Kushiro, I., 1970. Compositional relations of coexisting orthopyroxene, pigeonite and augite in a tholeiitic andesite from Hakone volcano. Contrib. Mineral. Petrol. 26, 265–275.

Nesbitt, H., Young, G., 1982. Early Proterozoic climates and plate motions inferred from major elements chemistry of lutites. Nature 299, 715–717.

Nisbet, E., Pearce, J., 1977. Clinopyroxene composition in mafic lavas from different tectonic settings. Contrib. Mineral. Petrol. 63, 149–160.

Parfenoff, A., Pomerol, Ch., Tourenq, J., 1970. Les minéraux lourds en grains. Méthodes d'étude et Détermination. In: Masson (Ed.), Paris, 571 pp.

Pearce, J., Cann, J., 1973. Tectonic setting of basic volcanic rocks determined using trace element analyses. Earth Planet. Sci. Lett. 19, 290–300.

Pearce, J.A., Norry, M.J., 1979. Petrogenetic implications of Ti, Zr, Y and Nb variations in volcanic rocks. Contrib. Mineral. Petrol. 69, 33–47.

Pearce, J., Harris, N., Tindle, A., 1984. Trace element discrimination diagrams for the tectonic interpretation of granitic rocks. J. Petrol. 25, 956–983.

Pettijohn, F., Potter, P., Siever, R., 1972. Sand and Sandstones Springer-Verlag, New York.

Pichavant, M., Kontak, D., Valencia, J., Clark, A., 1988a. The Miocene–Pliocene Macusani volcanics, SE Peru: I. Mineralogy and magmatic evolution of a two-mica aluminosilicate-bearing ignimbrite suite. Contrib. Mineral. Petrol. 100, 300–324.

Pichavant, M., Kontak, D., Briqueu, L., Valencia, J., Clark, A., 1988b. The Miocene–Pliocene Macusani volcanics, SE Peru: II. Geochemistry and origin of a felsic peraluminous magma. Contrib. Mineral. Petrol. 100, 325–338.

Pinto, L., 1999. Evolución tectónica y geomorfológica de la deformación cenozoica del borde occidental del Altiplano y su registro sedimentario entre los 19°08′ –19°27′ S (Región de Tarapacá, Chile). Memoria de Título y Tesis de Grado de Magister, Mención Geología. Universidad de Chile, Santiago 125 pp.

Pinto, L., Hérail, G., Charrier, R., (in press). Sedimentación sintectónica asociada a la deformación neógena en el borde oriental de la Depresión Central en la zona de Moquella (19°15'S, Norte de Chile). Revista Geológica de Chile.

Redwood, S.D., Rice, C.M., 1997. Petrogenesis of Miocene basic shoshonitic lavas in the Bolivian Andes and implications for hydrothermal gold, silver and tin deposits. J. South Am. Earth Sci. 10 (3–4), 203–221.

Rochat, Ph., 2002. Structures et Cinémathique de l'Altiplano nord-bolivien au sein des Andes Centrales. Mémoire H.S. N° 38, IRD (eds.) Univ. Joseph Fourier, Grenoble. 193 pp.

Rochat, Ph., Hérail, G., Baby, P., Aranibar, O., Mascle, G., 1998. Analyse géométrique et modèle tectonosédimentaire de l'Altiplano nord bolivien. C.R. Acad. Sci. Fr. 327, 769–775.

Roser, B., Korsch, R., 1986. Determination of tectonic setting of sandstone–mudstone suites using SiO_2 content and K_2O/Na_2O ratio. J. Geol. 94, 635–650.

Salas, R., Kast, R., Montecinos, F., Salas, I., 1966. Geología y Recursos Minerales del Departamento de Arica. Provincia de Tarapacá. IIG, Santiago (Chile). Boletín N° 21, 119 pp.

Sébrier, M., Soler, P., 1991. Tectonics and magmatism in the Peruvian Andes from late Oligocene time to the Present. Spec. Pap.-Geol. Soc. Am. 265, 259–278.

Seguel, J.E., 1991. Informe sobre la Geología del Complejo Volcánico Mamuta-Guaichane. Precordillera de Iquique. I Región. Departamento de Geología, Universidad de Chile. Proyecto III (Inédito 1599), 38 pp.

Schneider, A., Halls, C., 1985. Chronology of eruptive processes and mineralization of the Frailes Karikari volcanic field, eastern Cordillera, Bolivia. Comun.-Dep. Geol.,Univ. Chile 35, 217–224.

Sempere, T., Hérail, G., Oller, J., 1988. Los aspectos estructurales y sedimentarios del Oroclino Boliviano. Proceedings 5th Congreso Geológico Chileno, Depto. Geología y Geofisica (Universidad de Chile), Santiago, vol. 1, pp. A127–A142.

Sirvas, J., Torres, E., 1966. Consideraciones geológicas de la zona noroeste de la provincia Pacajes. IBP, vol. 6. Depto. de La Paz, Bolivia, pp. 54–64.

Soler, P., Jiménez, N., 1993. Magmatic constraints upon the evolution of the Bolivian Andes since Late Oligocene times. Proceedings 2nd International Symposium on Andean Geodynamics, ORSTOM editions, Oxford, UK, pp. 447–451.

Thiéblemont, D., 1999. Discrimination entre magmatismes calco-alcalins mantellique et crustal: l'example des Andes. C.R. Acad. Sci. Paris 329, 243–250.

Thorpe, R.S., Francis, P.W., 1979. Variation in Andean andesite compositions and their petrogenetic significance. Tectonophysics 57, 53–70.

Thorpe, R.S., Francis, P.W., Hammill, M., Baker, M.C.W., 1982. The Andes. In: Thorpe, R.S. (Ed.), Andesites: Orogenic Andesites and Related Rocks. Wiley, Chichester, UK, pp. 187–206.

Tobar, A., Salas, I., Kast, I., 1968. Cuadrángulos Camaraca y Azapa, Provincia de Tarapacá. IIG, Carta Geol. Chile 19–20, 5–11.

Wilson, M., 1989. Igneous Petrogenesis. Chapman & Hall, London 466 pp.

Winchester, J., Floyd, P., 1977. Geochemical discrimination of different magma series and their differentiation products using immobile elements. Chem. Geol. 20, 325–343.

Wood, B.J., 1975. The application of thermodynamics to some subsolidus equilibria involving solid solutions. Fortschr. Mineral. 52, 21–45 (Spec. vol. Papers and Proc. 9th Gen. Meeting I.M.A., Berlin (West)-Regensberg).